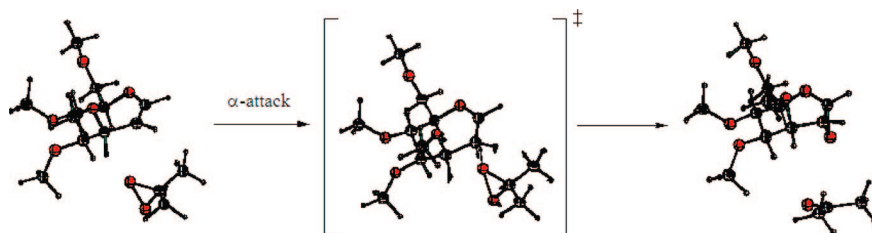# Stereoselectivity in the Epoxidation of Carbohydrate-Based Oxepines

Shankar D. Markad,[†] Shijing Xia,[‡] Nicole L. Snyder,[§,†] Bikash Surana,[†]
Martha D. Morton,[†] Christopher M. Hadad,*[,‡] and Mark W. Peczuh*[,†]

*Department of Chemistry, The University of Connecticut, 55 North Eagleville Road, Storrs, Connecticut
06269, and Department of Chemistry, The Ohio State University, 100 West 18th Avenue,
Columbus, Ohio 43210*

hadad.1@osu.edu; mark.peczuh@uconn.edu

Received May 12, 2008

The facial selectivity in the DMDO epoxidation of carbohydrate-based oxepines derived from glucose, galactose, and mannose has been determined by product analysis and density functional theory (DFT, B3LYP/6-31+G**//B3LYP/6-31G*) calculations. Oxepines **3** and **4**, derived from D-galactose and D-mannose, largely favor α- over β-epoxidation. The results reported here, along with selectivities in the DMDO-mediated epoxidation of D-xylose-based oxepine **1** and D-glucose-based oxepines **2** and **5** reported earlier, support a model in which electronic effects, guided by the stereochemistry of the oxygens on the oxepine ring, largely determine the stereoselectivity of epoxidation. Other contributing factors included conformational issues in the oxepine's transition state relative to the reactant, the asynchronicity in bond formation of the epoxide, and the overall steric bulk on the α- and β-faces of the oxepine. Considered together, these factors should generally predict facial selectivity in the DMDO-epoxidation of cyclic enol ethers.

1. Introduction

The formation of glycosidic linkages with use of 1,2-anhydrosugars as donors has enjoyed wide application in the syntheses of oligosaccharides and natural products.[1] Access to these donors from cyclic enol ether (glycals, for example) via epoxidation has been instrumental to their utilization. Because the cyclic enol ethers are often chiral, their reactions with achiral epoxidizing reagents can follow distinct stereochemical pathways which need not be equivalent. In fact, based on the stereochemistry of the cyclic enol ether, high selectivity in the formation of one anhydrosugar in preference to another is common.[2-5]

Our approach to the formation of glycosidic bonds in the septanose series has similarly relied on 1,2-anhydroseptanoses as a donor both directly[4,6,7] or indirectly through the formation of a thiophenyl septanoside.[8] Carbohydrate-based oxepines[9-11] have proven to be useful starting materials for preparing 1,2-anhydroseptanoses, with the oxepines acting as ring-expanded glycals. Selectivity observed in the epoxidation of carbohydrate-

---

[†] The University of Connecticut.

[‡] The Ohio State University.

[§] Current address: Department of Chemistry, Hamilton College, Clinton, NY 13323.

(1) (a) Seeberger, P. H.; Bilodeau, M. T.; Danishefsky, S. J. *Aldrichim. Acta* **1997**, *30*, 75. (b) Danishefsky, S. J.; Bilodeau, M. T. *Angew. Chem., Int. Ed. Engl.* **1996**, *35*, 1380.

(2) (a) Boulineau, F. P.; Wei, A. *J. Org. Chem.* **2004**, *69*, 3391. (b) Boulineau, F. P.; Wei, A. *Org. Lett.* **2002**, *4*, 2281. (c) Gervay, J.; Peterson, J. M.; Oriyama, T.; Danishefsky, S. J. *J. Org. Chem.* **1993**, *58*, 5465. (d) Marzabadi, C. H.; Spilling, C. D. *J. Org. Chem.* **1993**, *58*, 3761.

(3) (a) Majumder, U.; Cox, J. M.; Johnson, H. W. B.; Rainier, J. D. *Chem. Eur. J.* **2006**, *12*, 1736. (b) Kim, Y. J.; Wang, P. F.; Navarro-Villalobos, M.; Rohde, B. D.; Derryberry, J.; Gin, D. Y. *J. Am. Chem. Soc.* **2006**, *128*, 11906. (c) Rainier, J. D.; Allwein, S. P.; Cox, J. M. *J. Org. Chem.* **2001**, *66*, 1380.
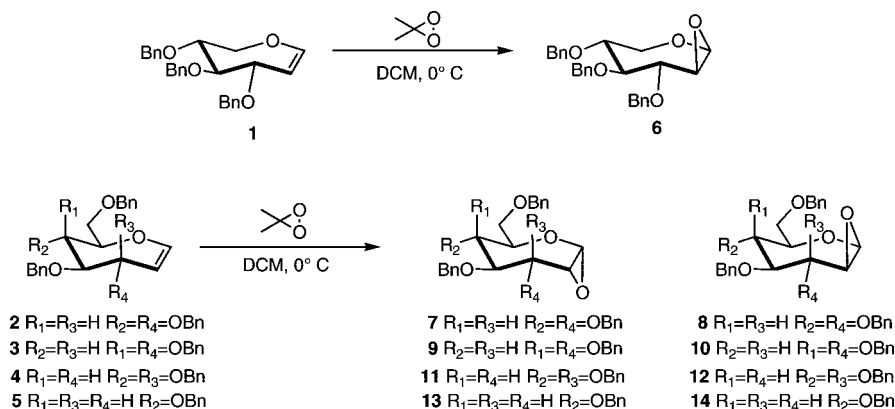
(4) Peczuh, M. W.; Snyder, N. L.; Fyvie, W. S. *Carbohydr. Res.* **2004**, *339*, 1163.

(5) Honda, E.; Gin, D. Y. *J. Am. Chem. Soc.* **2002**, *124*, 7343.

(6) DeMatteo, M.; Snyder, N. L.; Morton, M.; Baldisseri, D. M.; Hadad, C. M.; Peczuh, M. W. *J. Org. Chem.* **2005**, *70*, 24.

(7) DeMatteo, M.; Mei, S.; Fenton, R.; Morton, M.; Baldisseri, D. M.; Hadad, C. M.; Peczuh, M. W. *Carbohydr. Res.* **2006**, *341*, 2927.

SCHEME 1

SCHEME 2

based oxepines has been variable and was related to the specific starting material. For example, oxepine **1** was shown to selectively form the β-1,2-anhydroseptanose **6** when using dimethyldioxirane (DMDO) as the oxidant (Scheme 1). Selectivity in this system was determined by ^{1}H and ^{13}C NMR spectroscopy and by analysis of the methyl septanoside product that resulted from methanolysis of the 1,2-anhydroseptanose.[4] DMDO epoxidation of oxepine **2**, on the other hand, proved to be relatively unselective (**7:8** = 3:1, Scheme 1). In this case, the ratio of epoxides formed was quantified by characterizing the products of methanolysis.[6,7] Combined, these experiences prompted us to ask the question: What factors determine the selectivity in the epoxidation of carbohydrate-based oxepines? Herein, we analyze the outcomes of the DMDO oxidation of three related oxepines (**2**−**4**) by product analysis and density functional theory (DFT) calculations on the transition states in these reactions. Oxepines **2**, **3**, and **4** are derived from glucose, galactose, and mannose, respectively. The variation of stereochemistry about the ring allowed for an evaluation of the parameters that control the stereochemistry of epoxidation.

Recent reports on the epoxidation stereoselectivity of cyclic enol ethers from the Wei[12] and Rainier[13] laboratories influenced our perspective. Wei described a polarized-π frontier molecular orbital (PPFMO) model that explained selectivity in DMDO epoxidation of a series of 4-deoxypentenosides.[12] In their system, the reactant geometry was similar to that of the transition state, and C−O bond formation was asynchronous in the transition state. Repulsive electronic interactions between the heteroatoms of the ring substituents and the π-bond of the cyclic enol ether polarized the π-bond so that the nucleophilic π-bond had greater electron density on the face with fewer electronegative substituents. This gave rise to the idea of the facial selectivity being due to a "majority rule". The Rainier model similarly emphasized transition state geometry and asynchronous bond formation during the epoxidation of six- and seven-membered-ring cyclic enol ethers. Avoiding unfavorable interactions between DMDO and the allylic C−H bond in the transition state formed the basis for epoxidation selectivity in
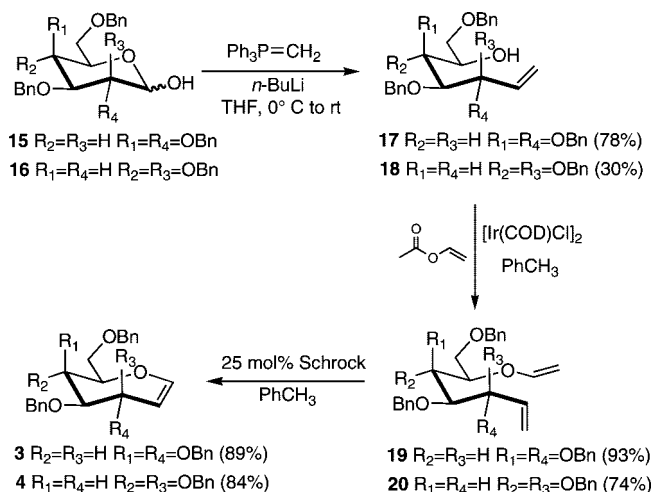
the systems they evaluated.[14] We were interested in evaluating these models in terms of the DMDO epoxidations of carbohydrate-based oxepines **1**−**5**.

2. Results and Discussion

2.1. DMDO Epoxidations of Carbohydrate-Based Oxepines. Oxepines **1**−**5** served as the starting materials for the DMDO epoxidation reactions. We have previously reported on the details for the synthesis of **1**, **2**, and **5** by a ring-closing methathesis (RCM)-based strategy.[4,6,11] Two new oxepines, **3** and **4**, were prepared by the same route but with a minor modification. Scheme 2 shows the synthesis of **3** and **4** from tetra-*O*-benzyl-D-*galacto*-pyranose **15** and tetra-*O*-benzyl-D-*manno*-pyranose **16**. Wittig methylenation[15] of the lactols gave δ-hydroxy alkenes **17** and **18** in 78% and 30% yields, respectively.[16] The change in synthetic sequence relative to our previous route came in the formation of vinyl ethers **19** and **20**. Vinyl etherification of the hydroxyl group on **17** was carried out with Pd(OAc)2 and ethyl vinyl ether[17] to give diene **19** with

(8) Castro, S.; Fyvie, W. S.; Peczuh, M. W. *Org. Lett.* **2005**, *7*, 4709.

(9) Castro, S.; Peczuh, M. W. *J. Org. Chem.* **2005**, *70*, 3312.

(10) Alcázar, E.; Pletcher, J. M.; McDonald, F. E. *Org. Lett.* **2004**, *6*, 3877.

(11) Peczuh, M. W.; Snyder, N. L. *Tetrahedron Lett.* **2003**, *44*, 4057.

(12) Cheng, G.; Boulineau, F. P.; Liew, S.-T.; Shi, Q.; Wenthold, P. G.; Wei, A. *Org. Lett.* **2006**, *8*, 4545.

(13) Orendt, A. M.; Roberts, S. W.; Rainier, J. D. *J. Org. Chem.* **2006**, *71*, 5565.
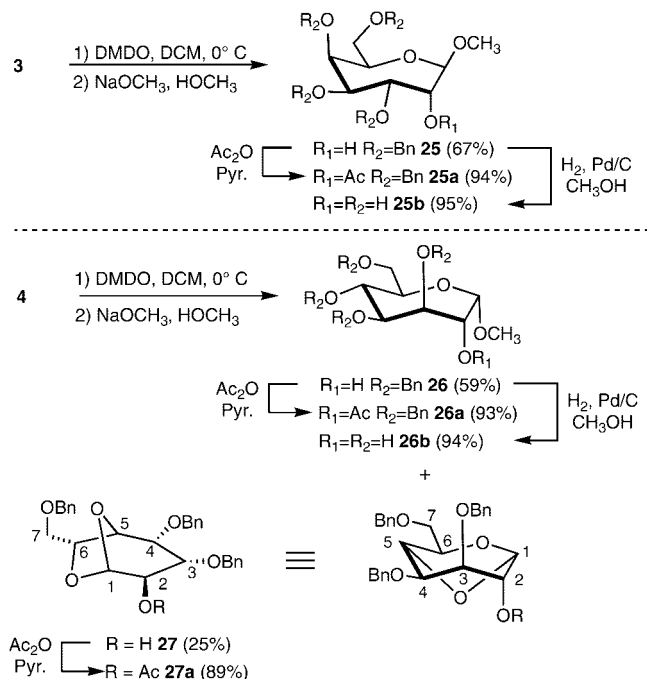
(14) Ando, K.; Green, N. S.; Li, Y.; Houk, K. N. *J. Am. Chem. Soc.* **1999**, *121*, 5334.

(15) Martin, O. R.; Saavedra, O. M.; Xie, F.; Liu, L.; Picasso, S.; Vogel, P.; Kizu, H.; Asano, N. *Bioorg. Med. Chem.* **2001**, *9*, 1269.

(16) Attempts to optimize the olefination of tetra-*O*-benzyl-D-*manno*-pyranose were unsuccessful. Elimination of benzyloxy substituents may be a competing reaction. See, for example: Callam, C. S.; Lowary, T. L. *J. Org. Chem.* **2001**, *66*, 8961.

(17) Handerson, S.; Schlaf, M. *Org. Lett.* **2002**, *4*, 407.

SCHEME 3

TABLE 1. Experimental Epoxidation Selectivities and Yields for 1−5

oxepine	epoxides (α:β)	products (α:β)	combined yield (%)	C1 ^{13}C δ (ppm)
1	6 (1:25)	21	89[a]	106.2 (21b)
2	7:8 (3:1)	22:23 (1:3)	63[b]	106.2 (22b); 110.0 (23b)
3	9:10 (25:1)	25	67	110.1 (25b)
4	11:12 (>25:1)	26:27 (7:3)	84	100.7 (26b)
5	13:14 (ND)	24	61[c]	112.2 (24b)

[a] These data are taken from ref 4. [b] These data are taken from ref 6. [c] These data are taken from ref 20.
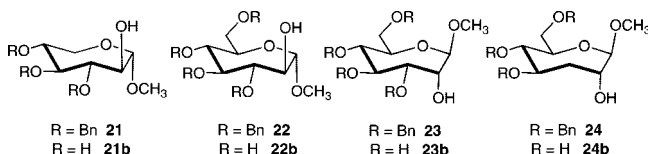
2.2. Stereochemical Characterization of the Reaction Products. Assignment of accurate structures to the products previously obtained in the epoxidation/methanolysis sequence was critical to understanding the stereoselectivity of the epoxidation reaction. The C2 group consistently reports on this selectivity and is insensitive to any subsequent epimerization/ anomerization. The stereochemistry of **21** was assigned by comparison to a known compound from Stevens.[21] Assignment of structures **22** and **23** was concurrent with a conformational analysis of the completely deprotected methyl septanosides corresponding to them.[6] The conformational analysis was in part used to define the stereochemistry in these two structures.

Evidence supporting our structural assignment of the new products has come from X-ray crystallography on methyl 3,4: 5,7-di-*O*-isopropylidene β-D-*glycero*-D-*galacto*-septanoside **29** (Figure 1). This molecule was prepared from the di-*O*-isopropylidene protected oxepine **28** via the DMDO/methanolysis sequence in 84% yield (Scheme 4). Deprotection of the acetonide groups in **29** provided methyl β-D-*glycero*-D-*galacto*-septanoside **29b** in 93% yield. Hydrogenolysis of **25** and **26** provided methyl β-D-*glycero*-L-*manno*-septanoside **25b** and methyl α-D-*glycero*-D-*galacto*-septanoside **26b** in 95% and 94% yield (Scheme 3). In addition to the protected septanosides **25**, **26**, and **29**, these deprotected methyl septanosides were utilized in the overall assignment of stereochemistry for the new molecules reported here.

In general, we have observed a partitioning of C1 ^{13}C chemical shifts in methyl septanosides based on the stereochemistry at the anomeric position, especially for completely deprotected methyl septanosides (Table 1).[7,22,23] The C1 ^{13}C chemical shifts for methyl α-septanosides range from 100 to 106 ppm whereas ^{13}C chemical shifts for methyl β-septanosides range from 110 to 112 ppm. On the basis of this trend, **25b** and **29b** fit into the range for β-septanosides with ^{13}C δ for C1 of 110.1 and 110.8 ppm, respectively. The NMR analysis was in accordance with the X-ray structure in the case of **29/29b**. Septanoside **26b**, on the other hand, gave a C1 δ of 100.7 ppm, indicating that its anomeric stereochemistry was α. With confidence in the C1 stereochemical assignment, we used an analysis of the ^3J coupling constants to assign the remaining C2 stereochemistry in the product structures.

very poor conversion even after refluxing the reaction mixture for several days. To improve the yield in the vinyl etherification reaction, an alternative method with an iridium catalyst as reported by Okimoto et al.[18] was used. Thus, treatment of δ-hydroxy alkene **17** with 10 mol % of [Ir(COD)Cl]₂ and vinyl acetate gave diene **19** in 93% yield. The mannose-derived diene **20** was prepared in 74% yield from **18** with use of the same reaction conditions. RCM, using 25 mol % of Schrock catalyst,[19] with **19** and **20** gave oxepines **3** and **4** in 89% and 84% yield, respectively.

As had previously been done for oxepines **1**, **2**, and **5**, the products from basic methanolysis of anhydroseptanoses derived from **3**, **4**, and **5** were analyzed to determine the selectivity of the DMDO epoxidation reaction. For example, methyl α-D-*ido*-septanoside **21** was the product of the epoxidation/methanolysis sequence for **1**, indicating that epoxidation occurred on the β-face of the oxepine. Under the same reaction conditions, oxepine **2** gave rise to methyl α-D-*glycero*-D-*ido*-septanoside **22** and methyl β-D-*glycero*-D-*gulo*-septanoside **23** (1:3 α:β) indicating only a slight preference for α-epoxide formation. C3 deoxygenated oxepine **5** provided β-septanoside **24**[20] through α-1,2-anhydroseptanose **13**, even in the absence of an allylic substituent. Subjecting galactose-derived oxepine **3** to the standard reaction conditions provided only the methyl β-septanoside product **25** in 67% overall yield (Scheme 3). Oxepine **4** showed more complex reactivity, giving methyl α-septanoside **26** and the cyclized product **27** in a combined yield of 84%. On the basis of these product structures, epoxidation of **3** and **4** occurred with high selectivity for the α-face (>25:1) of these oxepines. A complete rationale for the product structures in Scheme 3 is provided below. Results for all of the experimental epoxidation/methanolysis reactions are given in Table 1.

(18) Okimoto, Y.; Sakaguchi, S.; Ishii, Y. *J. Am. Chem. Soc.* **2002**, *124*, 1590.
(19) Schrock, R. R. *Tetrahedron* **1999**, *55*, 8141.
(20) Castro, S.; Duff, M.; Snyder, N.; Morton, M.; Kumar, C. V.; Peczuh, M. W. *Org. Biomol. Chem* **2005**, *3*, 3869.

(21) Tran, T. Q.; Stevens, J. D. *Aust. J. Chem.* **2002**, *55*, 171.
(22) We have also reported the crystal structure of an α-septanoside. See ref 9.
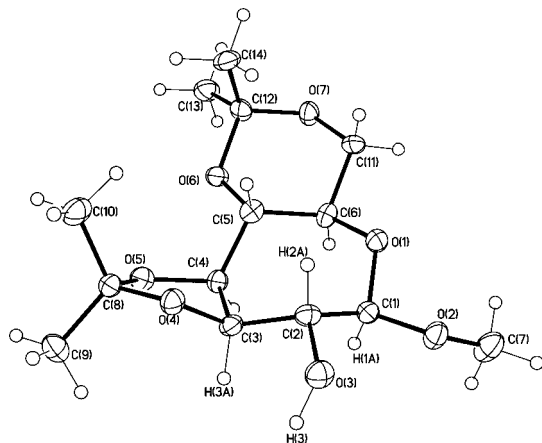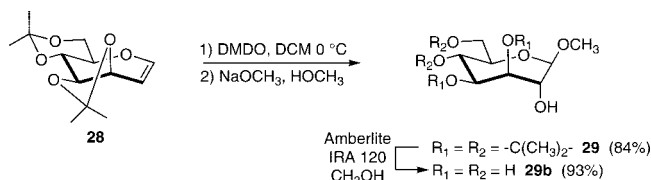(23) See the Supporting Information for a complete table of C1 chemical shifts.

FIGURE 1. ORTEP representation of **29** from X-ray data.

SCHEME 4


In addition to the X-ray and ^{13}C data, analysis of COSY/NOESY spectra of **25b**, **26b**, and **29b**, along with their AMBER-minimized structures, further supports the stereochemical assignment.[24] Diagnostic NOESY cross-peaks in the spectrum of **25b** are the H1−H4 and H1−H6 cross-peaks. These two transannular cross-peaks are estimated to be 2.4 and 2.1 Å in the calculated structure. For **26b**, the COSY spectrum shows only weak coupling between H1−H2 ($^3J_{H1,H2} = 3$ Hz from ^1H NMR). The NOESY spectrum, however, clearly shows an H1−H2 cross-peak. The calculated structure for **26b** puts the H1−H2 protons approximately 2.3 Å apart and on the same side/face of the ring. The magnitude of the H1−H2 cross-peak is similar to that of the H1-aglycon methyl (−OCH$_3$) NOE, which is also calculated to be in close proximity (2.3 Å). Other important NOEs observed for **26b** are H2 to H3 and H4 to H6. Calculated distances between these protons were 2.3 and 2.6 Å. Combined, these data strongly suggest the structure of **26b** to the 1,2-*cis* structure as shown. ^1H NMR signals for **29b** were less disperse than those for **25b**, but assignments could still be made. The NOESY spectrum of **29b** showed cross-peaks between H1 and the aglycon methyl (−OCH$_3$), H1 and H6, and H4 and H6. Interproton distances from the AMBER-minimized structure for **29b** again agree with these observations (2.4−2.6 Å). Overall, the collected crystallographic and spectroscopic data render a consistent picture for the structures of methyl septanosides **25**, **26**, and **29**.

We arrived at the structure for **27** by consideration of the reaction mechanism in combination with NMR experiments. Our previous observation of the intramolecular cyclization of an activated oxepine via its C5 benzyloxy group gave us additional perspective.[25] By considering the potential reaction mechanisms (Scheme 5), there could be five possible reaction paths for

anhydroseptanose **11**, three that invoke the anhydrosugar directly and two that proceed via cyclic oxonium ion **33**. The paths are the following: (a) attack of the C3 OBn oxygen to form a C2−C3 epoxide **30**; (b) attack of the C4 OBn oxygen atom to form the bicyclic product **31**; (c) attack of the C7 OBn oxygen atom to form the bicyclic product **32**; (d) attack by methoxide/methanol on the α-face of oxonium ion **33** to form methyl α-septanoside **26**; and (e) attack of the C5 OBn oxygen to the α-face of **33** to form **27**.

Product analysis showed pathway d to be the preferred course of the reaction, giving **26** in 55% yield. Both the ^1H and ^{13}C NMR spectra of the other product, **27** (25%), clearly showed that it was not a methyl septanoside. Notable differences were the lack of an indicative methyl glycoside singlet and also the absence of signals for one of the benzyl groups present in **4** and **11**. Further, the ^1H NMR and ^{13}C NMR did not show signals in the epoxide region, ruling out **30** as the product. HMBC NMR of **27a** showed correlation of H1 to carbons C3, C5, and C6 (all are three-bond couplings), and similarly, C1 correlated to H5 and H3. Also, C4 and C7 both show correlations with benzyl protons in the HMBC while C5 does not. This suggests that the benzyloxy substituent at C5 was the nucleophile, and not the corresponding groups at either C4 or C7. In total, correlations are consistent with **27**, but inconsistent with **31** or **32**.[26]

Structure **27** arises from attack of the C5 OBn oxygen onto the C1 of oxonium ion **33**. We have reported on similar reactivity of a C5 OBn oxygen in the NIS-mediated intramolecular cyclization of oxepine **1**. The bicyclic structure formed in that reaction (**34**) is reminiscent of **27**.[25] The nucleophilicity of the C5 OBn group likely relies on the electronic effects of the group, the stability of the corresponding benzyl/tropylium cation released in the reaction, and the proximity of the reacting groups. Both of the observed products in the epoxidation/methanolysis of **4** (**26** and **27**) arise from a presumed cyclic oxonium ion intermediate **33**. This is in contrast to the other products of methoxide attack on 1,2-anhydroseptanoses, where the products have arisen from S_N2 ring-opening of the epoxide. Although invoking oxonium ion **33** is speculative considering the reaction conditions of the methanolysis (NaOCH$_3$/HOCH$_3$), it is consistent with both products that have been characterized.[27]
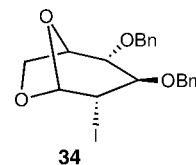
2.3. Transition State Calculations for DMDO Epoxidations. The product analyses above established the selectivity in epoxide formation for oxepines **1−5** and **28**. We were interested in developing a model for predicting the stereoselectivity of epoxidation in these systems and turned to computational chemistry for insight.

In this computational study, the selectivity of the DMDO-mediated epoxidations of the α- and β-faces of the oxepines was investigated at the B3LYP/6-31+G**//B3LYP/6-31G* level of theory.[28–31] Solvation effects were investigated by using the

(24) Spectra (COSY/NOESY), tabulated interproton distances, and the AMBER minimized structures for **25b**, **26b**, and **29b** are in the Supporting Information.

(25) Fyvie, W. S.; Morton, M.; Peczuh, M. W. *Carbohydr. Res.* **2004**, *339*, 2363.

(26) Full NMR spectral characterization (^1H, ^{13}C, COSY, HMQC, HMBC) for **27a** can be found in the Supporting Information.

(27) An investigation aimed at understanding the facility in forming oxonium **33** from **4** is currently underway.

(28) Parr, R. G.; Yang, W. *Density Functional Theory in Atoms and Molecules*; Oxford University Press: New York, 1989.

SCHEME 5
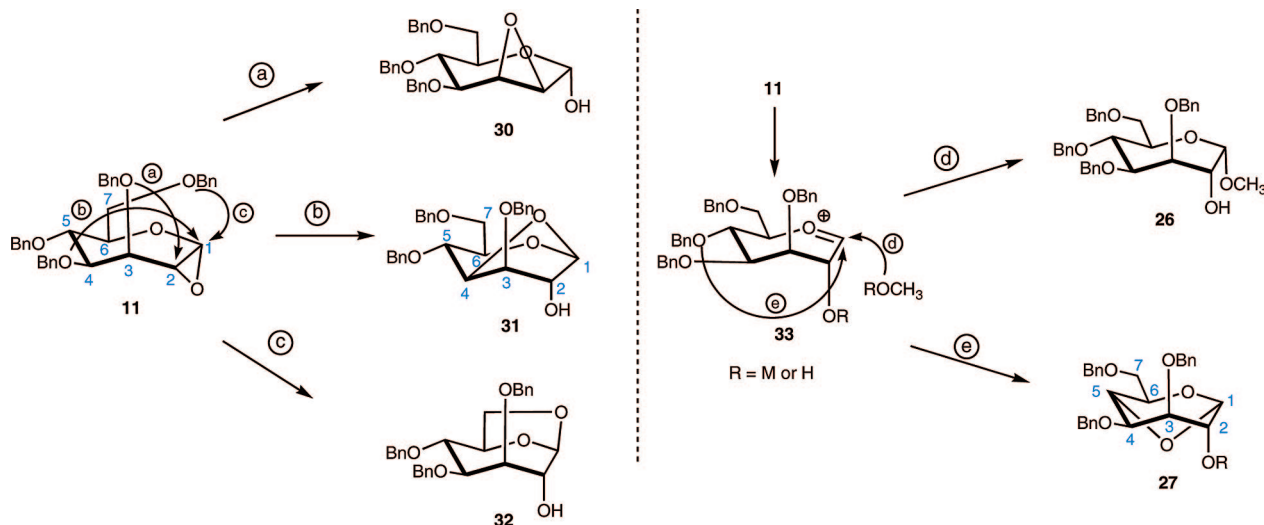
polarizable continuum model (PCM),[32–35] using single-point energy (B3LYP/6-31+G**) calculations with the gas-phase (B3LYP/6-31G*) optimized geometries. (*Note: For the subsequent discussion, we will refer to the B3LYP/6-31+G**//B3LYP/6-31G* level simply as B3LYP, unless otherwise noted.*) Despite changes in the relative ordering of different conformers or transition states, the general trends between the free energies and enthalpies are relatively consistent—all of the energies are provided in the Supporting Information. In the subsequent discussion, the free energies will be presented.

To simplify the computational study, the model systems (**2a**, **3a**, and **4a**—Table 2) with four methoxy substituents were evaluated instead of the experimental systems (**2**, **3**, and **4**) that had benzyloxy substituents at the C3, C4, C5, and C7 positions. By replacing a phenyl group with a hydrogen atom, we anticipate that the **2a**, **3a**, and **4a** models would underestimate the steric effect between the substituents and DMDO; however, this replacement was significantly more computationally tractable for locating and characterizing transition states.

We began the investigation of the facial selectivity by first considering the conformational flexibility of the three model compounds **2a**–**4a**. Using the OPLS-AA force field,[36] we performed a conformational search using a Monte–Carlo protocol available in MacroModel,[37] and for the different compounds, many conformations within ~3.5 kcal/mol of the global minimum were obtained: 20 conformers for **2a**, 25 conformers for **3a**, and 43 conformers for **4a**. These unique conformations were then fully optimized at the B3LYP/6-31G* level of theory with use of Gaussian03.[38] After this subsequent

refinement, there were 4 unique conformers for **2a**, 3 unique conformers for **3a**, and 5 unique conformers for **4a**; all of these had relative free energies within ~1 kcal/mol of the respective global minimum at the B3LYP level in each case.

The calculated energetic parameters for the low-energy conformers of **2a**, **3a**, and **4a** are shown in Table 2 at the OPLS-AA and the B3LYP level. The B3LYP level predicted a different global minimum from that predicted by the OPLS-AA force field for **2a** and **3a**. For **4a**, even though these two methods predicted the same global minimum, the ordering of the low-energy conformations was different based on these two methods.[39] A similar tendency was observed in our previous study.[7] The geometrical parameters for the OPLS-AA and B3LYP/6-31G* optimized structures are very similar, and obviously structural differences are not critical for the energetic trends by the different computational methods. Our previous study stated that the nature of the difference between molecular mechanics (AMBER*) and electronic structure (HF/6-31G*) methods appeared to be their treatment of important hydrogen-bonding interactions.[7] However, in these systems, hydrogen-bonding interactions are not possible. Therefore, the nature of the difference between the OPLS-AA and the B3LYP methods arises from other interactions.

The low-energy conformers of the **2a** and **3a** had very similar geometries with a $^5C_{1,2}$ conformation being preferred for the ring (Table 2). The differences between these conformers are related to the orientation of the methoxy substituent on the C3–C7 positions. The low-energy conformers of **4a**, however, possessed unique conformations of the seven-membered ring, including $^5C_{1,2}$, $^{1,2}C_5$, and $^{5,6}TC_{3,4}$ isomers (Table 2).

To predict the facial selectivity for epoxidation as suggested by Wei,[12] we computed the electrostatic potential (ESP) of the most stable conformer of each oxepine (Table 3), in order to assess a preference for reactivity based on this easily computed diagnostic for the oxepine. The α-face and β-face views of the electron density surface, mapping the values of the electrostatic potential (red–blue corresponding to ESP values of −0.01 to +0.01 au), are depicted for the most stable conformer (**2a**-A, **3a**-A, and **4a**-A) in each model system.

As shown in Table 3 for **2a**-A, **3a**-A, and **4a**-A, the α-face had a smaller magnitude of negative charge than the β-face for

(29) Labanowski, J. W.; Andzelm, J. *Density Functional Methods in Chemistry*; Springer: New York, 1991.

(30) Becke, A. D. *J. Chem. Phys.* **1993**, *98*, 5648.

(31) Lee, C.; Yang, W.; Parr, R. G. *Phys. Rev. B* **1988**, *37*, 785.

(32) Miertus, S.; Scrocco, E.; Tomasi, J. *Chem. Phys.* **1981**, *55*, 117.

(33) Cammi, R.; Tomasi, J. *J. Comput. Chem.* **1995**, *16*, 1449.

(34) Tomasi, J.; Persico, M. *Chem. Rev.* **1994**, *94*, 2027.

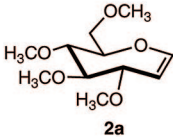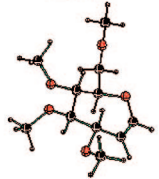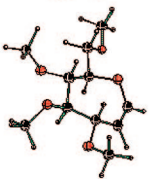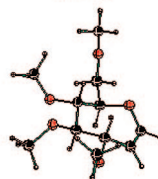(35) Cramer, C. J.; Truhlar, D. G. *Chem. Rev.* **1999**, *99*, 2161.
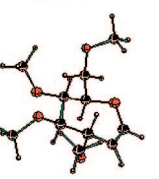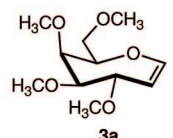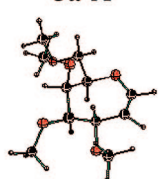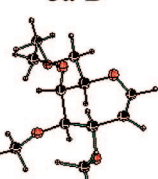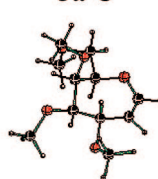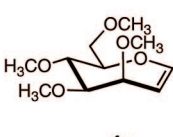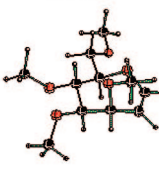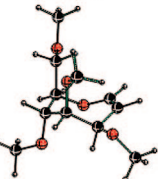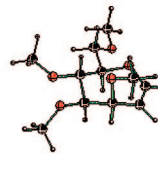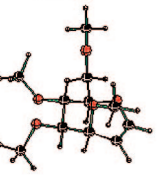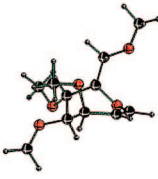
(36) Jorgensen, W. L.; Maxwell, D. S.; Tirado-Rives, J. *J. Am. Chem. Soc.* **1996**, *118*, 11225.

(37) (a) Osawa, E.; Musso, H. *Angew. Chem., Int. Ed. Engl.* **1983**, *22*, 1. (b) Halgren, T. A. *J. Am. Chem. Soc.* **1992**, *114*, 7827. (c) Halgren, T. A. *J. Comput. Chem.* **1996**, *17*, 616. (d) Mohamadi, F.; Richards, N. G. J.; Guida, W. C.; Liskamp, R.; Lipton, M.; Caufield, C.; Chang, G.; Hendrickson, T.; Still, W. C. *J. Comput. Chem.* **1990**, *11*, 440.

(38) Frisch, M. J. et al. Gaussian 03, Revision B.04; Gaussian, Inc.: Pittsburgh, PA, 2003.

(39) See the Supporting Information for details.

TABLE 2.   Calculated Energetic Parameters for the Low-Energy Conformers of 2a, 3a, and 4a: The Relative Energies (ΔE_{rel}, kcal/mol) with the OPLS-AA Force Field and the Relative Free Energies at 298 K ($\Delta G_{298,rel}$, kcal/mol) at the B3LYP/6-31+G**//B3LYP/6-31G* Level of Theory[a]

Oxepine		Conformers			
		2a-A	**2a**-B	**2a**-C	**2a**-D
OPLS-AA E_{rel}		1.4	0.0	1.8	3.3
B3LYP $G_{298, rel}$		0.0	0.1	0.5	0.7
		3a-A	**3a**-B	**3a**-C	
OPLS-AA E_{rel}		0.8	1.2	3.0	
B3LYP $G_{298, rel}$		0.0	0.4	1.0	
		4a-A	**4a**-B	**4a**-C	**4a**-D	**4a**-E
OPLS-AA E_{rel}		0.0	2.0	0.1	2.2	1.4
B3LYP $G_{298, rel}$		0.0	0.3	0.5	0.6	0.6

[a] All of the energies are relative to the corresponding global minimum for each molecule.

all three oxepines, although the difference was not large. It is well accepted that epoxidation appears to involve electrophilic addition to the alkene.[40,41] The ESP results would suggest a β-face preference for the DMDO epoxidation. This prediction is opposite from the experimental results. While asserting transition state preferences from ground state properties is obviously questionable, it is often synthetically convenient. The disparity between the calculated ESP results and the experimentally observed selectivities indicated that the facial preferences of the transition states were different from the ground state preferences for these carbohydrate-based oxepines. Therefore, to quantitatively predict the facial selectivity, the thermodynamics of the reaction pathways, including comprehensive structural and energetic evaluations of the diastereomeric transition states, were completed. These transition state calculations also considered the different conformations available for each oxepine.

The atomic charges of the transition states and reactant complexes for all of the DMDO epoxidations with the model systems (**2a**, **3a**, and **4a**) were obtained by using a natural population analysis (NPA)[42] at the B3LYP level of theory. For all of the DMDO epoxidations of the various conformers, the NPA results show that negative charge accumulates on the transferring O of DMDO upon progressing from the reactant complexes to the transition states. This indicates that DMDO epoxidations involve electrophilic addition to the double bond of the oxepine, a trend that is consistent with previous studies.[41] On the basis of the NPA results, C2 has a negative charge, in general, and C1, due to the bonded ring oxygen, has a positive charge, and suggests that the C2$\cdots$O bond would form first for the eventual epoxide in an asynchronous transition state for epoxidation.[39]

The DMDO epoxidations on the α- and β-faces of the most stable conformers of **2a**, **3a**, and **4a** were studied at the gas-phase B3LYP level. The transition state for each pathway was located and then connected to its respective reactant complexes (RC) and products (P). Energetic values for all of the stationary points for α/β facial attack of DMDO with the different

(40) Lynch, B. M.; Pausacker, K. H. *J. Chem. Soc.* **1955**, 1525.
(41) Miaskiewicz, K.; Smith, D. A. *J. Am. Chem. Soc.* **1998**, *120*, 1872.

(42) (a) Reed, A. E.; Weinstock, R. B.; Weinhold, F. *J. Chem. Phys.* **1985**, *83*, 735. (b) Reed, A. E.; Weinhold, F.; Curtiss, J. A. *Chem. Rev.* **1988**, *88*, 899.

TABLE 3. The α-Face and β-Face Views of the Electrostatic Potential (Red to Blue Corresponding to Charge Values of −0.01 to +0.01 au) for the Most Stable Conformers of 2a, 3a, and 4a at the B3LYP/6-31G* Level of Theory in the Gas Phase

Oxepine-Conformer	α-face[a]	β-face[a]
2a-A		
3a-A		
4a-A		

[a] The double bond of the oxepine is located at the bottom of each contour plot.

	α-attack		
	RC	TS	P
ΔG_{298}	9.9	23.5	-48.5

	β-attack		
	RC	TS	P
ΔG_{298}	11.2	24.8	-47.0
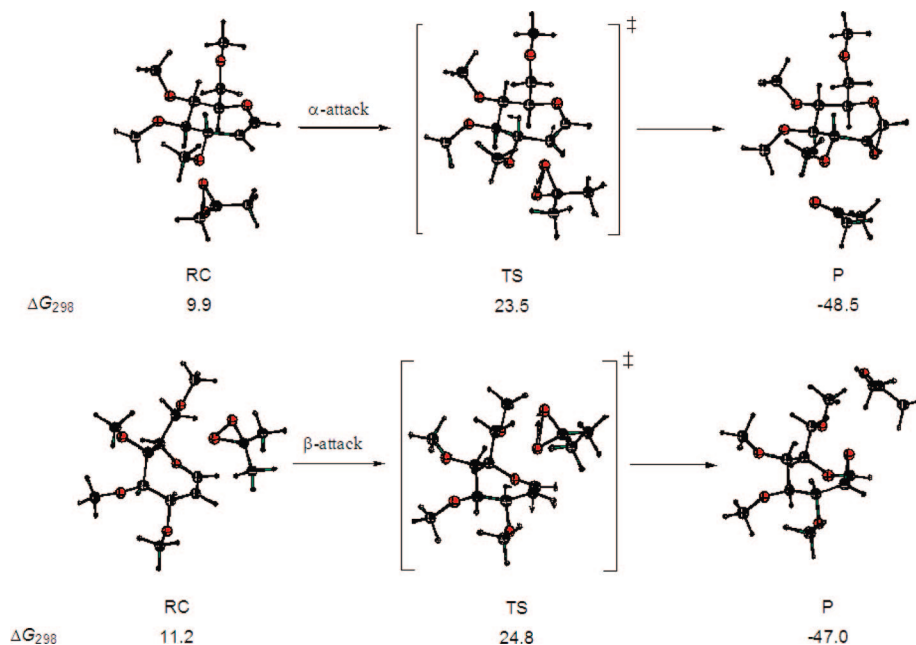
FIGURE 2. Relative free energies at 298 K (ΔG_{298}, kcal/mol) of the most favorable DMDO epoxidations on the α- and β-faces of **2a** at the B3LYP/6-31+G**//B3LYP/6-31G* level of theory. All of the energies are relative to the infinitely separated DMDO and the most stable conformer of **2a**.

conformers are listed in the Supporting Information. The energies are presented as relative to the infinitely separated DMDO and the most stable conformer. Considering the effect of implicit solvation with the PCM did not significantly alter the calculated results relative to experiment, therefore, only the gas-phase results are presented here.[43]

The calculated results of the most favorable pathways for the DMDO epoxidations on the α- and β-faces of **2a** are shown in Figure 2. Among these low-energy conformers (**2a**-A, **2a**-B, **2a**-C, and **2a**-D), **2a**-C underwent the most favorable pathway for the DMDO epoxidation on the α-face of **2a**, while **2a**-B provided that on the β-face of **2a**.[39] The DMDO epoxidation on either face was highly exoergic. As shown in Table 4, the free energy of activation for the α-face epoxidation was about

(43) All of the PCM results are presented in the Supporting Information.

TABLE 4. Difference in the Free Energies of Activation at 298 K ($\delta\Delta G^{\ddagger}$, kcal/mol) and the Ratios of the DMDO Epoxidations on the α- and β-Faces of 2a, 3a, and 4a from Our Computational and Experimental Studies

	theoretical (B3LYP/6-31+G**//B3LYP/6-31G*)[a]				exptl[b]
	α-TS (conf.)	β-TS (conf.)	$\delta\Delta G^{\ddagger}\beta-\alpha$	Facial selectivity (α:β)[c]	Facial selectivity (α:β)
2a	2a-C ($^5C_{1,2}$)	2a-B ($^{5,6}TB_{3,4}$)	1.3	80:20	3:1
3a	3a-B ($^5C_{1,2}$)	3a-B (envelope)	4.6	99.2:0.8	>25:1
4a	4a-D ($^5C_{1,2}$)	4a-A ($^5C_{1,2}$)	9.0	100:0	>25:1

[a] Gas-phase calculations at the B3LYP/6-31+G**//B3LYP/6-31G* level of theory (kcal/mol). [b] In this study. [c] Based on calculated $\delta\Delta G^{\ddagger}$ values.
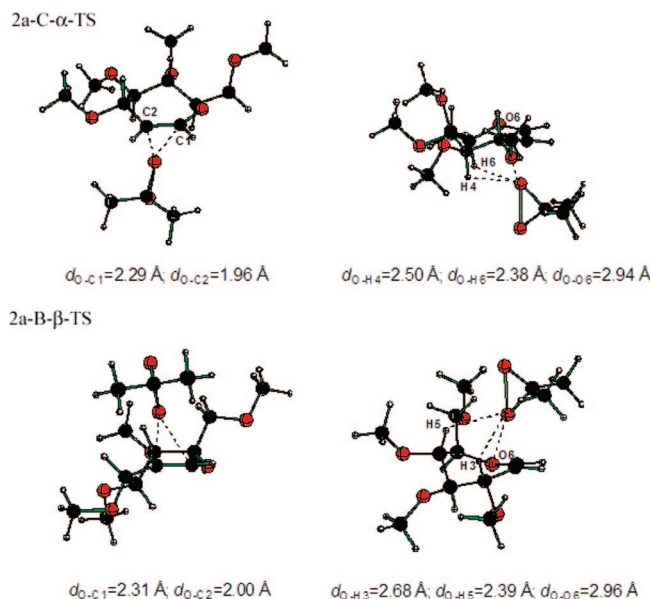
FIGURE 3. Front and side views of the transition state geometries of the most favorable DMDO epoxidations on the α- and β-faces of 2a, based on the B3LYP/6-31G* calculations.

1.3 kcal/mol lower than that for the β-face. Thus the formation of the α-epoxide is favored kinetically over the β-epoxidation (4:1 α:β). From the calculated $\delta\Delta G^{\ddagger}$ values, the calculated ratio for the α/β facial selectivity by DMDO for 2a is very similar to our experimental results (3:1 α:β) for the benzyloxy-substituted 2.

The α-face epoxidation transition states for the four conformers of 2a have very similar $^5C_{1,2}$ ring conformations to the starting oxepine; however, those on the β-face adopt a novel ($^{5,6}TB_{3,4}$) conformation (Figure 3). In all cases, the geometric search for each transition state started with a $^5C_{1,2}$ ring structure.[39] No significant differences in the distances between the axial hydrogens and the approaching oxygen could be determined for the epoxidation transition states of the α- and β-faces, and CH⋯O hydrogen bonding did not contribute to the preference for the α-face epoxidation. As shown in Figure 3, the transition state geometries for the most favorable DMDO epoxidations on the α- and β-faces of 2a showed a significant difference in torsional strain. The β-face epoxidation of 2a proceeded through a transition state with a $^{5,6}TB_{3,4}$ ring conformation, which most likely sacrificed some torsional strain to avoid the electrostatic interaction between lone-pair electrons on the incoming oxygen and those on O6 of the oxepine. The more demanding torsional strain for the β-face transition

structure probably rationalizes the energetic preference for the α-face epoxidation in 2a. The epoxidation on either face proceeded through a transition state with an asynchronous spiro geometry for which the C2⋯O bond forms first (Figure 3). This transition state could minimize the electrostatic interaction between the lone-pair electrons on the incoming DMDO oxygen and those on O6 of the oxepine. We thus postulate that O6 plays an important role in the transition state and also for dictating the α-facial kinetic selectivity.

The calculated results of the most favorable pathway for the DMDO epoxidations on either face of 3a are shown in Figure 4. Among three low-energy conformers (3a-A, 3a-B, and 3a-C), the 3a-B conformer underwent the most favorable pathway for the DMDO epoxidation on either face of 3a.[39] Similar to 2a, the epoxidation on either face of 3a was highly exoergic. The calculated free energy of activation for the epoxidation of the α-face of 3a was 4.6 kcal/mol lower than that for the β-face; thus, the α-facial selectivity was more significant for 3a (130:1 α:β) than for 2a (4:1 α:β), as shown in Table 4. Once again, the calculated ratio for α:β facial selectivity for methyl-substituted 3a is very consistent with our experimental results (>25:1 α:β) for benzyloxy-substituted 3.

For the three low-energy conformers of 3a, the transition states of the α-face epoxidation reactions had very similar conformations as their corresponding conformers with a $^5C_{1,2}$ ring structure. During the β-facial attack, the oxepines again adopted novel ring structures, specifically envelope-like conformations.[39] In the α-face transition state (Figure 5), the C1 and C2 positions did not deviate much from the plane, which consists of C3, C4, C6, and O6. Only C5 was displaced from the plane of the other six ring atoms. Similar to 2a, CH⋯O hydrogen bonding did not contribute to the preference for the α-face epoxidation. On the other hand, the β-face epoxidation of 3a proceeded through a transition state with an envelope-like ring conformation, which appears to have sacrificed some significant torsional strain to avoid the electrostatic interaction between the lone-pair electrons on the incoming oxygen of DMDO and those on O6 of the oxepine. However, for this envelope conformation, there are still some electrostatic interactions between the unpaired electrons on O5 and on the incoming O of DMDO, thereby contributing to the α-facial selectively. Similar to 2a, the epoxidation on either face of 3a proceeded through a transition state with an asynchronous spirocyclic geometry. For 3a, O6 appears to play an important role in the formation of the asynchronous transition state, while O5 and O6 seem to control the facial selectivity.

The calculated results of the most favorable pathways for the DMDO epoxidation on the α- and β-faces of 4a are shown in Figure 6. Among the five low-energy conformers (4a-A through 4a-E), the 4a-D conformer underwent the most favorable pathway for the α-facial epoxidations, while the 4a-A conformer provided that preference for the β-face.[44] In a similar manner as for 2a and 3a, the epoxidation reactions on either face of 4a were highly exoergic. The calculated free energy of activation for epoxidation of the α-face of 4a was 9.0 kcal/mol lower than that for the β-face; thus, the DMDO epoxidation should only occur to the α-face of 4a (100:0 α:β) as shown in Table 4. The computational results for the model compound 4a are once again very consistent with our experimental ratio
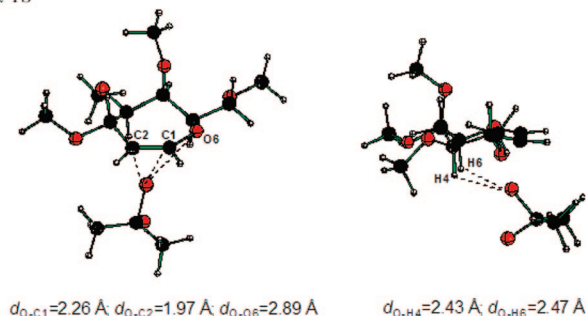
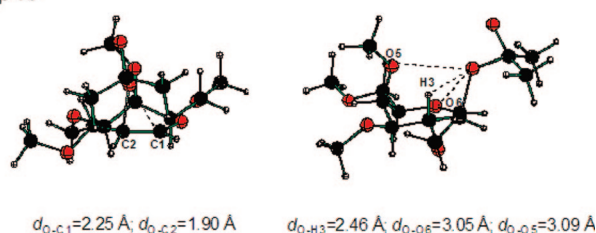(44) The transition states of the DMDO epoxidation of 4a-B and 4a-E could not be found.
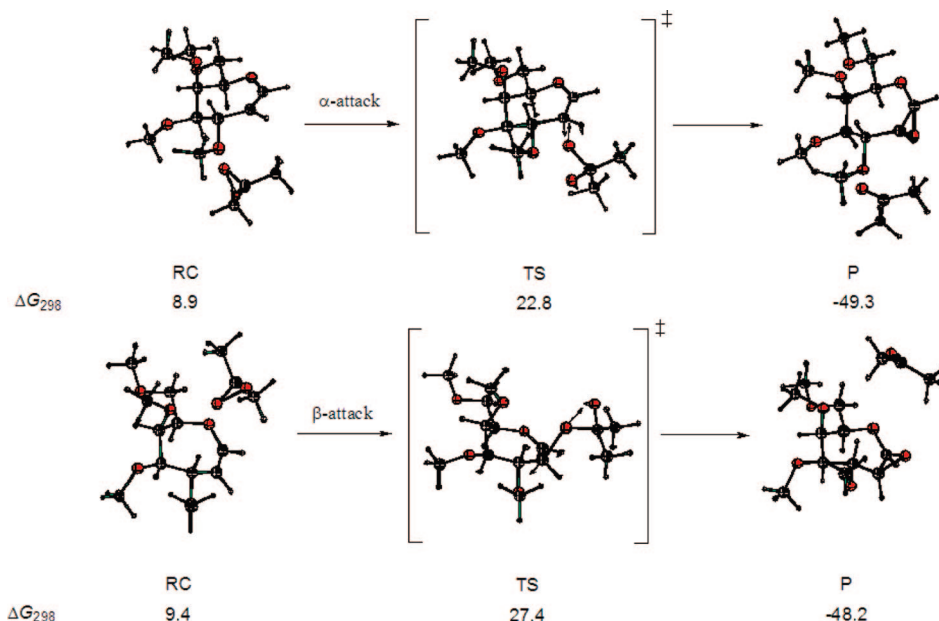
FIGURE 4. The relative free energies at 298 K (ΔG_{298}, kcal/mol) of the most favorable DMDO epoxidations on the α- and β-faces of **3a** at the B3LYP/6-31+G**//B3LYP/6-31G* level of theory. All of the energies are relative to the infinite separated DMDO and most stable conformer of **3a**.

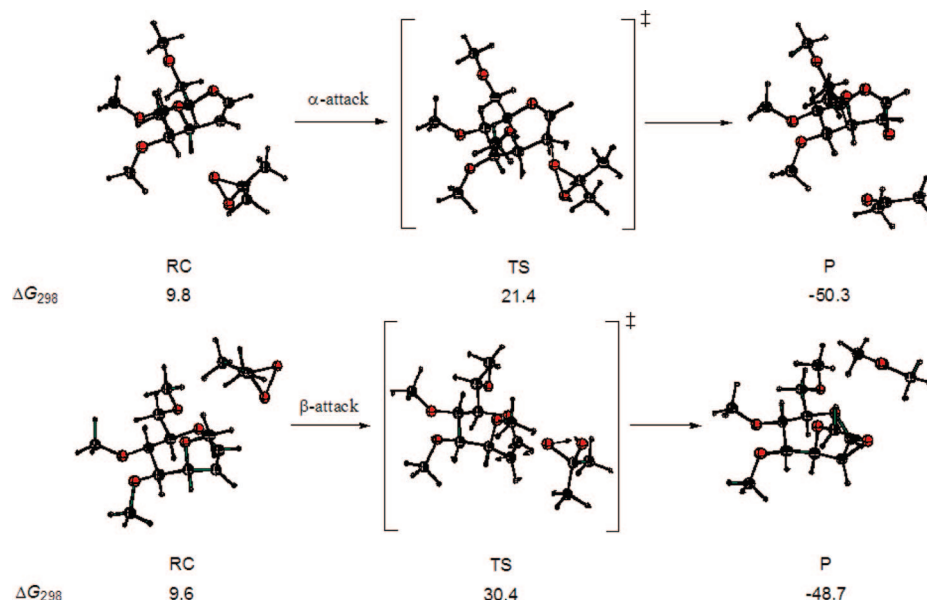**FIGURE 5.** Front and side views of the transition state geometries of the most favorable DMDO epoxidations on the α- and β-faces of **3a**, based on the B3LYP/6-31G* optimizations.

for the α:β facial selectivity (>25:1 α:β) for benzyloxy-substituted **4**.

For the five low-energy conformers of **4a**, the epoxidation transition states on either face had very similar conformations as their corresponding starting conformers ($^5C_{1,2}$, $^{1,2}C_5$, and $^{5,6}TC_{3,4}$).[39] This was different from the cases of the other two oxepines, **2a** and **3a**. Similar to **2a** and **3a**, however, CH···O hydrogen bonding did not contribute to the preference for the α-facial epoxidation. Because the transition state geometries for the DMDO epoxidations on the α- and β-faces of **4a** did not show any obvious difference in their structures (Figure 3), torsional strain does not appear to be the main contribution to the high preference for the α-facial selectivity. By carefully

analyzing the geometries of the α-TS and β-TS structures, we believe that the most significant contribution for the α-facial preference was the electrostatic interaction between the lone-pair electrons on the incoming oxygen of DMDO and those on O3 and O6 of the oxepine. To avoid the electrostatic interaction between the unpaired electrons on O3 and the incoming O of DMDO, a $^5C_{1,2}$ ring conformation is adopted in the transition state for β-facial epoxidation on **4a**. As shown in Figure 7, the O–O3 distance for **4a**-A-β-TS was only 2.79 Å, which was 0.3 Å shorter than the O–O5 distance in the **3a**-B-β-TS case. Similar as for **2a** and **3a**, the epoxidation on either face proceeded through a transition state with an asynchronous spiro geometry (Figure 7) in which the forming C1···O and C2···O distances are 2.41 and 1.99 Å, respectively, for the favored α-TS, while they are 2.25 and 1.92 Å, respectively, for the β-TS. For **4a**, it appears that O6 plays an important role in the formation of the asynchronous transition state, and O3 controls the facial selectivity.

2.4. Factors that Govern the Stereoselectivity of DMDO Epoxidations. The original impetus for this investigation was to determine the factors that govern selectivity in the epoxidation of carbohydrate-based oxepines. The agreement between the experimentally determined epoxidation selectivities for **2–4** and the computational results on **2a–4a** provides the basis for enumerating these factors. While there are both steric and electronic contributions to the observed selectivities, the ability of the less sterically demanding oxepines **2a–4a** to computationally reproduce the experimental data for the parent compounds **2–4** suggested that electronic factors predominate. By incorporating factors of the Wei "majority rule"[12] and the Rainier "asynchronicity rule",[13] a normative model for cyclic enol ether epoxidation develops. A list of key considerations includes the following: (i) the number and orientation of electronegative substituents on the ring relative to the reacting alkene [these factors are a reiteration of the majority rule]; (ii) reorganization of the transition state, driven by repulsive interactions between the ring oxygen of the oxepine (O6) and the O of DMDO, relative to the reactant; (iii) the overall

FIGURE 6. The relative free energies at 298 K (ΔG_{298}, kcal/mol) of the most favorable DMDO epoxidations on the α- and β-faces of **4a** at the B3LYP/6-31+G**//B3LYP/6-31G* level of theory. All of the energies are relative to the infinite separated DMDO and most stable conformer of **4a**.
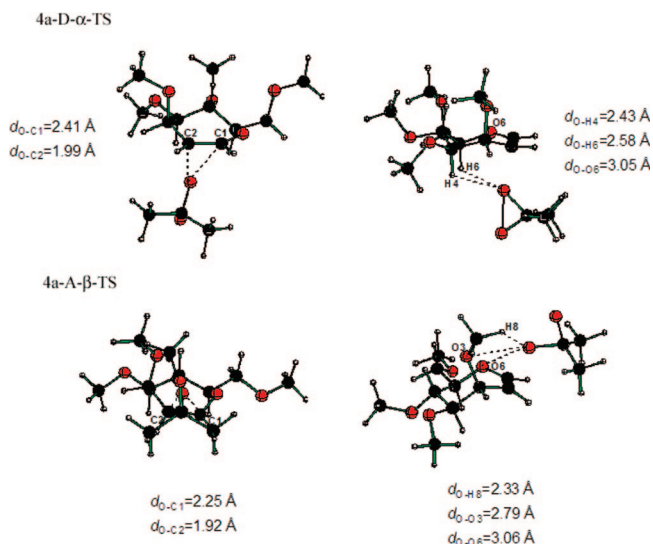
FIGURE 7. Front and side views of the transition state geometries of the most favorable DMDO epoxidations on the α- and β-faces of **4a**, based on the B3LYP/6-31G* optimizations.

synchronicity in epoxide bond formation; and (iv) the difference in the overall steric bulk on one side of the ring relative to the other. There is some overlap in these factors, but each is qualified in the proceeding paragraphs.

Application of the Wei majority rule to carbohydrate-based oxepines **2**–**4** allows qualitatively accurate prediction of epoxidation selectivities. This result suggests that the majority rule may be general for substituted cyclic enol ethers. For oxepines **2**–**4**, the orientation of the (protected) C7 hydroxymethyl group was considered among the electronegative substituents that would contribute to the majority rule. The overall electronegative effect may be attenuated due to its remote attachment to the ring, but it should contribute nonetheless. With this in mind, collecting substituents on the oxepines shows that **2** should give low selectivity, having two "α" substituents at C3 and C5, and two "β" substituents at C4 and C6; that is, for **2**, there should be no electronic majority rule. A similar tabulation for **3** and **4**

shows that there are more β substituents (C4, C5, and C6 for **3** and C3, C4, and C6 for **4**) giving rise to α-selectivity for epoxidation. The C3 deoxygenated oxepine **5** also preferentially formed the α-epoxide as evidenced by the formation of the methyl β-3-deoxy-D-*glycero*-D-*gulo*-septanoside **24**. For **5**, there are two β substituents (C4 and C6) and one α substituent (C5). The observed α-selective epoxidation for this system is in accordance with the majority rule. Oxepine **1**, which is the only oxepine that gives rise to β-facial selectivity, follows this analysis too. It has two α-benzyloxy substituents (C3 and C5) and only one β-benzyloxy group at C4. The majority rule is an electronic effect; the associated steric bulk of the benzyl protecting groups in these systems should also make a contribution to the observed selectivities. Wei[12] also used the PPFMO method to predict the facial selectivity for epoxidation of 4-deoxypentenosides; however, the validity of the predictions from PPFMO analysis depends strongly on the similarity between the reactant and transition state structures—a relationship that does not apply to the epoxidation of carbohydrate-based oxepines (**2a** and **3a**). In fact, the observed α-selectivity for epoxidation of **2** may solely reflect the increased steric bulk on the β-face of the oxepine due to the size of the protected hydroxymethyl group at C7 plus one benzyloxy group at C4 versus the two α-benzyloxy groups at C3 and C5.

Transition state reorganization and asynchronicity of bond formation in the epoxidation process also play a significant role in determining selectivities. The conformational reorganization observed in the computationally derived transition states for β-epoxidation of **2** and **3** contribute to the fact that these are energetically unfavorable routes; that reorganization for β-epoxidation of **4** was not seen is somewhat of a surprise. However, as a rationalization, we should note that in the β-epoxidation of **4**, the ring adopted a $^5C_{1,2}$ ring conformation to avoid repulsive electrostatic interactions between unpaired electrons on O6 and the incoming O of DMDO. In fact, the conformational reorganization in the β transition states for **2** and **3** is likely due to the minimization of the repulsive interaction between O6 and the O of DMDO. Anticipation of this repulsive

electronic interation between these oxygens for a given face of a cyclic enol ether allows predictive power in new systems. The asynchronous nature of the bond formation in the reaction plays a significant role for α- over β-epoxidation selectivity of **4**. That is because the pseudoaxial allylic substituent (C3) disfavors epoxidation on the same face based on electronic repulsion. While reorganization and asynchronicity are primarily electronic effects, the steric effects of the benzyl protecting groups also contribute here.

3. Conclusions

We have utilized density functional theory (B3LYP/6-31+G**//B3LYP/6-31G*) to explain the facial selectivity in DMDO-mediated epoxidation of carbohydrate-based oxepines. Through these combined experimental and theoretical treatments, a general model for predicting epoxidation outcomes for highly substituted cyclic enol ethers has been developed. The computational method can quantitatively predict the facial preference of these reactions. It can also provide the transition state structures that can be used to investigate the details of the interactions. In this study, the DMDO epoxidation reactions proceed through a transition state with an asynchronous spiro geometry, and proceed in an electrophilic manner for which the most electron-rich carbon center of the double bond attacks the transferring O of the DMDO oxidant. The lone-pair electrons on O6 prove to play an important role in the formation of the asynchronous transition state. Selectivity is determined by two major electronic factors. First, the collected electronegative substituents on one side or the other of the double bond favors attack on DMDO from the side with greater electron density (the side opposite to the majority of electronegative substituents). Second, the repulsive interaction between the O6 lone-pair electrons and the O of DMDO disfavors one transition over another. This repulsion can even distort the ring conformation of the oxepine in a disfavored transition state. The factors governing facial selectivity enumerated here should be applicable to substituted cyclic enol ethers generally.

4. Experimental Methods

1,6-Anhydro-3,4,5,7-tetra-*O*-benzyl-2-deoxy-D-*galacto*-sept-1-enitol (3). The synthesis was perfomed in a glovebox. To a solution of diene **19** (0.26 g, 0.46 mmol) in toluene (115 mL) was added Schrock catalyst (0.088 g, 0.115 mmol) and the resulting reaction mixture was stirred in the glovebox for 4 h. The reaction vessel was taken out from the glovebox and toluene was removed under reduced pressure to obtain a black residue, which gave **3** (0.22 g, 89%) as a thick liquid after column chromatography (hexanes/ethyl acetate = 9/1). R_f 0.52 (hexanes:EtOAc 7:3); [α]$_D^{22}$ +24.8 (*c* 3.88, CHCl$_3$). ^{1}H NMR (400 MHz, CDCl$_3$) δ 3.42 (dd, *J* = 9.0, 7.8 Hz, 1H), 3.56 (dd, *J* = 9.3, 6.4 Hz, 1H), 3.60 (d, *J* = 9.3 Hz, 1H), 3.80 (dd, *J* = 6.6, 6.4 Hz, 1H), 4.04 (s, 1H), 4.37 (AB, *J*$_{AB}$ = 11.9 Hz, 2H), 4.48 (dd, *J* = 6.5, 2.2 Hz, 1H), 4.66 (d, *J* = 11.8 Hz, 1H), 4.71–4.67 (m, 4H), 4.81 (d, *J* = 11.8 Hz, 1H), 4.91 (d, *J* = 11.8 Hz, 1H), 6.22 (dd, *J* = 8.0, 2.2 Hz, 1H), 7.23–7.38 (m, 20H); ^{13}C NMR (100 MHz, CDCl$_3$) δ 70.0, 72.9, 73.5, 73.7, 74.2, 74.7, 79.0, 85.4, 107.3, 127.8 (s), 127.9, 128.0, 128.1 (s), 128.5, 128.6 (s), 138.1, 138.6, 138.8, 144. ESI-MS *m/z* (M + Na)$^+$ calcd for C$_{35}$H$_{36}$O$_5$Na$^+$ 559.2455, found 559.2445.

1,6-Anhydro-3,4,5,7-tetra-*O*-benzyl-2-deoxy-D-*manno*-sept-1-enitol (4). The synthesis was perfomed in a glovebox. To a solution of diene **20** (0.44 g, 0.78 mmol) in toluene (190 mL) was added Schrock catalyst (0.149 g, 0.195 mmol) in toluene (10 mL) and the resulting solution was stirred in the glovebox for 4 h. Toluene was removed under reduced pressure and the residue was purified

by column chromatography (hexanes/ethyl acetate = 9/1) to give **4** (0.35 g, 84%) as a thick liquid. R_f 0.52 (hexanes:EtOAc = 8:2); [α]$_D^{22}$ −17.55 (*c* 1.0, CHCl$_3$). ^{1}H NMR (400 MHz, CDCl$_3$) δ 3.55 (dd, *J* = 10.8, 2.6 Hz, 1H), 3.59 (dd, *J* = 10.8, 5.6 Hz, 1H), 3.66 (dd, *J* = 9.8, 2.2 Hz, 1H), 3.92–4.01 (m, 2H), 4.18 (d, *J* = 11.4 Hz, 1H), 4.30 (d, *J* = 11.4 Hz, 1H), 4.47 (d, *J* = 12.3 Hz, 1H), 4.50 (d, *J* = 12.5 Hz, 1H), 4.56 (d, *J* = 12.3 Hz, 1H), 4.57 (d, *J* = 12.2 Hz, 1H), 4.60 (d, *J* = 1.8 Hz, 1H), 4.67 (d, *J* = 12.6 Hz, 1H), 4.73 (dt, *J* = 9.6, 1.8 Hz, 1H), 4.83 (d, *J* = 12.6 Hz, 1H), 6.42 (dd, *J* = 6.9, 2.2 Hz, 1H), 7.04–7.12 (m, 2H), 7.22–7.37 (m, 16H), 7.38–4.43 (m, 2H); ^{13}C NMR (100 MHz, CDCl$_3$) δ 70.2, 71.2, 72.1, 72.6, 73.3, 76.0, 77.7, 78.8, 105.4, 127.5, 227.5, 127.6, 127.8, 127.9, 127.9, 128.0, 128.3, 128.3, 128.4, 137.5, 138.2, 138.4, 138.8, 146.5. ESI-MS *m/z* (M + Na)$^+$ calcd for C$_{35}$H$_{36}$O$_5$Na$^+$ 559.2455, found 559.2441.

1,2-Anhydro-3,4,5,7-tetra-*O*-benzyl-α-D-*glycero*-L-*manno*-septanoside (9). Oxepine **3** (0.22 g, 0.41 mmol) was dried azeotropically with toluene (3 × 10 mL) under reduced pressure and then dissolved in dry DCM (12 mL) and cooled in an ice bath to 0 °C. DMDO (0.55 M) in DCM (2 × 0.88 mL) was added portion-wise and the mixture was stirred at 0 °C for 1 h. The solvent was removed under reduced pressure. ^{1}H NMR of the resulting material showed quantitative conversion (400 MHz, CDCl$_3$) δ 3.12 (d, *J* = 2.3 Hz, 1H), 3.44 (dd, *J* = 9.0, 8.4 Hz, 1H), 3.53 (dd, *J* = 8.7, 5.0 Hz, 1H), 3.75 (dd, *J* = 9.5, 1.3 Hz, 1H), 3.86 (dd, *J* = 8.1, 5.6 Hz, 1H), 3.96 (d, *J* = 0.9 Hz, 1H), 4.36–4.45 (m, 3H), 4.65–4.97 (m, 7H), 7.28–7.43 (m, 20H); ^{13}C NMR (100 MHz, CDCl$_3$) δ 58.7, 69.5, 70.7, 73.4, 74.0, 74.2 (s), 74.7, 76.8, 79.1, 84.1, 127.8, 127.9 (s), 128.0, 128.3, 128.5, 128.6, 128.7, 129.2, 138.2, 138.5, 138.8. ESI-MS *m/z* (M + Na)$^+$ calcd for C$_{35}$H$_{36}$O$_6$Na$^+$ 575.2404, found 575.2409.

1,2-Anhydro-3,4,5,7-tetra-*O*-benzyl-α-D-*glycero*-D-*galacto*-septanoside (11). Oxepine **4** (0.20 g, 0.37 mmol) was dried azeotropically with toluene (3 × 10 mL) and then dissolved in DCM (20 mL). DMDO (2.44 mL, 0.22 M) was added at 0 °C and the resulting reaction mixture was stirred for 1 h. The solvent was removed under reduced pressure to give a thick liquid in quantitative yield according to ^{1}H NMR. R_f = 0.35 (hexanes:EtOAc 6:4); [α]$_D^{22}$ +8.07 (*c* 2.1, CHCl$_3$). ^{1}H NMR (300 MHz, CDCl$_3$) δ 3.19 (br s, 1H), 3.65 (dd, *J* = 10.5, 3.3 Hz, 1H), 3.67 (dd, *J* = 8.1, 3.0 Hz, 1H), 3.83 (dd, *J* = 10.5, 5.7 Hz, 1H), 3.92–3.98 (m, 1H), 3.99–4.03 (m, 1H), 4.21 (d, *J* = 2.7 Hz, 1H), 4.30 (d, *J* = 11.4 Hz, 1H), 4.39 (d, *J* = 11.7 Hz, 1H), 4.54 (d, *J* = 12.0 Hz, 1H), 4.65 (d, *J* = 12.0 Hz, 1H), 4.66 (d, *J* = 12.3 Hz, 1H), 4.74 (d, *J* = 12.3 Hz, 1H), 4.82 (d, *J* = 12.0 Hz, 1H), 4.85 (d, *J* = 12.3 Hz, 1H), 4.96 (d, *J* = 2.7 Hz, 1H), 7.11–7.18 (m, 2H), 7.25–7.50 (m, 18H); ^{13}C NMR (75 MHz, CDCl$_3$) δ 59.2, 69.1, 71.6, 71.7, 71.8, 72.9, 73.1, 75.5, 77.8, 77.9, 80.0, 127.5 (s), 127.55, 127.58, 127.6 (s), 127.7 (s), 127.8, 128.28 (s), 128.3 (s), 128.33 (s), 128.9, 129.6, 137.5, 137.8, 138.0, 138.3.

3,4,5,7-Tetra-*O*-benzyl-1,2-dideoxy-D-*galacto*-hept-1-ene (17). To a suspension of H$_3$CPPh$_3$Br (0.46 g, 1.29 mmol) in dry THF (5 mL) at 0 °C was added *n*-BuLi (0.76 mL, 1.6 M in hexane) slowly over a period of 10 min and the resulting reaction mixture was stirred for 30 min at 0 °C and 30 min at room temperature. To a solution of *galacto* lactol **15** (0.2 g, 0.37 mmol) in THF (5 mL) was added *n*-BuLi (0.21 mL, 1.6 M in hexane) at 0 °C and the reaction mixture was stirred for 30 min. This solution was transferred to the ylide solution under N$_2$ at 0 °C and the resulting reaction mixture was stirred at room temperature for 55 h. The reaction mixture was quenched with saturated NH$_4$Cl (3 mL), THF was removed under reduced pressure, and then extracted with DCM (3 × 10 mL). Purification by column chromatography (hexanes/ethyl acetate = 9.5/0.5) gave a thick liquid (0.155 g, 78%). R_f 0.48 (hexanes:EtOAc 8:2). [α]$_D^{22}$ −4.03 (*c* 1.6, CHCl$_3$). ^{1}H NMR (400 MHz, CDCl$_3$) δ 3.07 (d, *J* = 8.0 Hz, D$_2$O exchangeable, 1H), 3.49–3.3.60 (m, 2H), 3.80–3.87 (m, 2H), 4.12 (dd, *J* = 8.0, 4.0 Hz, 1H), 4.16 (dd, *J* = 8.0, 4.0 Hz, 1H), 4.35–4.45 (m, 2H), 4.46 (d, *J* = 12.0 Hz, 1H), 4.53 (d, *J* = 12.0 Hz, 1H), 4.68 (d, *J* = 11.8

Hz, 1H), 4.71−4.78 (m, 1H), 4.79 (s, 2H), 5.33 (d, J = 8.0 Hz, 1H), 5.38 (d, J = 16.0 Hz, 1H), 5.90 (ddd, J = 16.0, 7.9, 2.5 Hz, 1H), 7.20−7.42 (m, 20H); ^{13}C NMR (100 MHz, CDCl$_3$) δ 69.7, 70.3, 71.2, 73.08, 73.14, 75.2, 76.6, 80.8, 82.1, 119.1, 127.5 (s), 127.6 (s), 127.7 (s), 128.0 (s), 128.1 (s), 128.3 (s), 135.7, 138.0, 138.1, 138.2. ESI-MS m/z (M + Na)$^+$ calcd for C$_{35}$H$_{38}$O$_5$Na$^+$ 561.2611, found 561.2594.

3,4,5,7-Tetra-*O*-benzyl-1,2-dideoxy-D-*manno*-hept-1-ene (18). To a solution of lactol **16** (1.4 g, 2.59 mmol) in THF (15 mL) was added *n*-BuLi (1.7 mL, 1.6 M) at −10 °C and the resulting solution was stirred for 30 min at 0 °C. To a solution of Ph$_3$PCH$_3$Br (3.24 g, 9.06 mmol) was added *n*-BuLi (1.6 M, 5.67 mL) at −20 °C and the resulting solution was allowed to warm to 0 °C and stirred for 30 min. The ylide solution was added to the lactol via cannula at −20 °C and stirred for 24 h at rt. Saturated NH$_4$Cl (5 mL) was added and THF was removed under reduced pressure. The residue was dissolved in DCM (40 mL) and washed with water and brine. The DCM layer was dried and solvent removed under reduced pressure. Purification of the resulting material by column chromatography (hexanes/ethyl acetate = 9/1) gave a thick liquid (0.42 g, 30%). R_f 0.59 (hexanes:EtOAc 7:3). [α]$_D^{22}$ +6.38 (*c* 1.55, CHCl$_3$). ^{1}H NMR (400 MHz, CDCl$_3$) δ 2.64 (d, J = 5.8 Hz, 1H, D$_2$O exchangeable), 3.56 (dd, J = 9.6, 5.4 Hz, 1H), 3.62 (dd, J = 9.6, 3.4 Hz, 1H), 3.83−3.91 (m, 2H), 3.96−4.04 (m, 1H), 4.11 (d, J = 7.4 Hz, 1H), 4.24 (d, J = 11.7 Hz, 1H), 4.47 (s, 2H), 4.48 (d, J = 11.1 Hz, 1H), 4.49 (d, J = 11.2 Hz, 1H), 4.60 (d, J = 11.3 Hz, 1H), 4.62 (d, J = 11.1 Hz, 1H), 4.71 (d, J = 11.2 Hz, 1H), 5.39 (dd, J = 8.8, 1.5 Hz, 1H), 5.42 (d, J = 17.3 Hz, 1H), 5.94 (ddd, J = 17.6, 7.8, 2.4 Hz, 1H), 7.17−7.38 (m, 20H); ^{13}C NMR (100 MHz, CDCl$_3$) δ 69.9, 70.2, 71.3, 73.3, 73.9, 74.3, 78.6, 80.3, 80.9, 119.7, 127.47, 127.54, 127.66, 127.7, 127.8, 127.84, 128.2, 128.21, 128.3, 128.4, 136.2, 138.0, 138.4, 138.5. ESI-MS m/z (M + Na)$^+$ calcd for C$_{35}$H$_{38}$O$_5$Na$^+$ 561.2611, found 561.2615.

3,4,5,7-Tetra-*O*-benzyl-1,2-dideoxy-6-*O*-vinyl-D-*galacto*-hept-1-ene (19). Ethyl vinyl ether (75 mL) and DCM (5 mL) were combined in a flame-dried round-bottomed flask. To this mixture was added 1,10-phenanthroline (0.098 g, 0.54 mmol) followed by Pd(OAc)$_2$ (0.121 g, 0.54 mmol) with stirring for 15 min. To this mixture was added alcohol **17** (1.95 g, 3.62 mmol) in DCM (20 mL) and the resulting reaction mixture was refluxed for 10 d. The solvent was removed under reduced pressure. The residue was directly loaded on a column and purified (hexanes/ethyl acetate = 9.5/0.5) to give a thick liquid **19** (0.27 g, 13%) in 59% yield based on 0.46 g, conversion. R_f 0.64 (hexanes:EtOAc 8:2). Repeated attempts at obtaining HRMS data for **19** provided only the product of vinyl ether hydrolysis (**17**). [α]$_D^{22}$ +6.87 (*c* 5.39, CHCl$_3$). ^{1}H NMR (400 MHz, CDCl$_3$) δ 3.59 (dd, J = 9.8, 6.4 Hz, 1H), 3.65 (dd, J = 9.8, 5.9 Hz, 1H), 3.75 (dd, J = 8.0, 3.2 Hz, 1H), 3.99 (dd, J = 6.5, 1.6 Hz, 1H), 4.03 (dd, J = 8.0, 2.7 Hz, 1H), 4.18 (dd, J = 7.8, 3.1 Hz, 1H), 4.32 (d, J = 12.0 Hz, 1H), 4.30−4.34 (m, 1H), 4.37 (dd, J = 14.1, 1.6 Hz, 1H), 4.42 (s, 2H), 4.43 (AB, J_{AB} = 12.0 Hz, 2H), 4.62 (d, J = 12.0 Hz, 1H), 4.65 (d, J = 12.0 Hz, 1H), 4.70 (d, J = 12.0 Hz, 1H), 5.29 (d, J = 11.3 Hz, 1H), 5.38 (d, J = 17.4 Hz, 1H), 6.00 (ddd, J = 17.8, 7.7, 2.6 Hz, 1H), 6.36 (dd, J = 14.0, 6.5 Hz, 1H), 7.16−7.36 (m, 20H); ^{13}C NMR (100 MHz, CDCl$_3$) δ 68.6, 69.9, 72.9, 73.8, 74.4, 76.9, 77.2, 79.8, 80.9, 88.3, 118.4, 127.2, 127.23 (s), 127.3 (s), 127.33, 127.4 (s), 127.6 (s), 127.62 (s), 127.68 (s), 127.95 (s), 128.0 (s), 128.1, 128.2, 136.3, 137.7, 138.1, 138.2, 138.23, 151.6.

3,4,5,7-Tetra-*O*-benzyl-1,2-dideoxy-6-*O*-vinyl-D-*galacto*-hept-1-ene (19). To a solution of **17** (0.1 g, 0.186 mmol) in toluene (5 mL) was added [Ir(cod)Cl]$_2$ (0.012 g, 0.018 mmol), Na$_2$CO$_3$ (0.013 g, 0.113 mmol), and vinyl acetate (0.33 g, 3.72 mmol). The solution was heated to 100 °C and stirred for 12 h. Toluene was removed under reduced pressure and the residue was extracted with DCM (3 × 10 mL). Purification by column chromatography (hexanes/ethyl acetate = 9.5/0.5) gave a thick liquid **19** (0.098 g, 93%). The physical and analytical data were found to be identical as given above.

3,4,5,7-Tetra-*O*-benzyl-1,2-dideoxy-6-*O*-vinyl-D-*manno*-hept-1-ene (20). To a solution of alcohol **18** (0.58 g, 1.08 mmol) in toluene (20 mL) was added [Ir(cod)Cl]$_2$ (0.072 g, 0.11 mmol), Na$_2$CO$_3$ (0.069 g, 0.65 mmol), and vinyl acetate (0.2 mL, 21.6 mmol). The solution was heated to 100 °C and stirred for 15 h. Toluene was removed under reduced pressure and the residue was extracted with DCM (3 × 10 mL). Column chromatography of the residue (hexanes/ethyl acetate = 9.5/0.5) gave a thick liquid **20** (0.451 g, 74%). R_f 0.57 (hexanes:EtOAc 8:2). [α]$_D^{22}$ −1.56 (*c* 0.9, CHCl$_3$). ^{1}H NMR (400 MHz, CDCl$_3$) δ 3.67 (dd, J = 10.8, 5.0 Hz, 1H), 3.78 (dd, J = 7.0, 3.5 Hz, 1H), 3.84 (dd, J = 10.8, 2.6 Hz, 1H), 4.02 (dd, J = 6.5, 1.6 Hz, 1H), 4.08 (t, J = 7.7 Hz, 1H), 4.09 (dd, J = 7.0, 3.5 Hz, 1H), 4.16−4.20 (m, 1H), 4.24 (d, J = 11.6 Hz, 1H), 4.34 (dd, J = 14.0, 1.6 Hz, 1H), 4.49 (s, 2H), 4.51 (d, J = 11.3 Hz, 1H), 4.55 (d, J = 11.4 Hz, 1H), 4.56 (d, J = 11.5 Hz, 1H), 4.59 (d, J = 12.3 Hz, 1H), 4.70 (d, J = 11.0 Hz, 1H), 5.39 (d, J = 8.6 Hz, 1H), 5.43 (d, J = 15.7 Hz, 1H), 5.96 (ddd, J = 17.6, 7.9, 2.4 Hz, 1H), 6.30 (dd, J = 14.1, 6.5 Hz, 1H), 7.20−7.32 (m, 20H); ^{13}C NMR (100 MHz, CDCl$_3$) δ 68.9, 69.9, 73.3, 74.4, 74.43, 77.8, 78.7, 80.4, 81.0, 89.2, 119.8, 127.37, 127.42, 127.59, 127.61, 127.7, 128.0, 128.1, 128.2, 128.3, 136.3, 138.2, 138.4, 138.6, 138.7, 151.0. ESI-MS m/z (M + Na)$^+$ calcd for C$_{37}$H$_{40}$O$_5$Na$^+$ 587.2768, found 587.2768.

Methyl-3,4,5,7-tetra-*O*-benzyl-β-D-*glycero*-L-*manno*-septanoside (25). To a solution of epoxide **9** in CH$_3$OH (5 mL) was added NaOCH$_3$ (20 mg) at 0 °C and the mixture was stirred overnight at rt. The reaction was quenched by adding saturated NH$_4$Cl (2 mL) and volatiles were removed under reduced pressure. The residue was dissolved in DCM (10 mL) and washed with H$_2$O. The DCM layer was dried and solvent was removed under reduced pressure. Purification of this material by column chromatography (hexanes/ethyl acetate = 7/3) gave β-methyl septanoside **25** (0.16 g, 67% overall). R_f 0.59 (hexanes:EtOAc 1:1). [α]$_D^{22}$ +41.9 (*c* 3.38, CHCl$_3$). ^{1}H NMR (400 MHz, CDCl$_3$) δ 2.84 (d, J = 1.6 Hz, 1H), 3.43 (s, 3H), 3.59−3.73 (m, 3H), 3.83 (dd, J = 8.9, 1.5 Hz, 1H), 3.97−4.02 (m, 2H), 4.23 (d, J = 6.4 Hz, 1H), 4.30 (d, J = 8.9, 4.4 Hz, 1H), 4.48 (AB, J_{AB} = 11.8 Hz, 2H), 4.58−4.68 (m, 3H), 4.82 (d, J = 12.0 Hz, 1H), 4.84 (d, J = 12.0 Hz, 1H), 4.95 (d, J = 11.6 Hz, 1H), 7.24−7.35 (m, 20H); ^{13}C NMR (100 MHz, CDCl$_3$) δ 55.9, 69.9, 73.6, 73.7, 74.1, 74.41, 74.44, 75.6, 77.2, 79.1, 79.5, 79.6, 108.1, 127.48 (s), 127.50 (s), 127.7 (s), 127.8 (s), 127.9 (s), 128.1 (s), 128.2 (s), 128.3 (s), 128.4 (s), 138.1, 138.2, 138.6, 138.7. ESI-MS m/z (M + Na)$^+$ calcd for C$_{36}$H$_{40}$O$_7$Na$^+$ 607.2666, found 607.2642.

2-*O*-Acetyl-3,4,5,7-tetra-*O*-benzylmethyl-β-D-*glycero*-L-*manno*-septanoside (25a). To a solution of **25** (0.05 g, 0.086 mmol) in pyridine (0.068 g, 6.5 mmol) was added Ac$_2$O (0.26 g, 2.56 mmol) and DMAP (2 mg) and the mixture was stirred for 15 h at rt. Volatiles were removed under reduced pressure and the reaction mixture was purified by column chromatography (hexanes/ethyl acetate = 9/1) to give **25a** (0.05 g, 94%). R_f 0.51 (hexanes:EtOAc 7:3); [α]$_D^{22}$ −29.13 (*c* 0.7, CHCl$_3$). ^{1}H NMR (300 MHz, CDCl$_3$) δ 2.08 (s, 3H), 3.39 (s, 3H), 3.62 (dd, J = 9.8, 5.4 Hz, 1H), 3.68 (dd, J = 9.8, 6.8 Hz, 1H), 3.77−3.82 (m, 1H), 3.84 (dd, J = 8.4, 2.1 Hz, 1H), 3.97 (t, J = 2.4 Hz, 1H), 4.31 (dd, J = 8.5, 3.6 Hz, 1H), 4.35 (d, J = 5.8 Hz, 1H), 4.45 (AB, J_{AB} = 11.8 Hz, 2H), 4.52 (d, J = 11.7 Hz, 1H), 4.60 (d, J = 12.0 Hz, 1H), 4.62 (d, J = 12.0 Hz, 1H), 4.63 (d, J = 11.7 Hz, 1H), 4.82 (d, J = 12.0 Hz, 1H), 4.86 (d, J = 11.7 Hz, 1H), 5.49 (dd, J = 5.8, 3.6 Hz, 1H), 7.18−7.34 (m, 20H); ^{13}C NMR (75 MHz, CDCl$_3$) δ 21.1, 55.8, 70.0, 73.4, 73.6, 73.9, 74.0, 74.4, 75.2, 78.1, 78.4, 78.9, 105.6, 127.4, 17.6, 127.61, 127.8, 127.9, 128.1, 128.13, 128.2, 128.3, 169.6. ESI-MS m/z (M + Na)$^+$ calcd for C$_{38}$H$_{42}$O$_8$Na$^+$ 649.2772, found 649.2771.

Methyl-3,4,5,7-tetra-*O*-benzyl-α-D-*glycero*-D-*galacto*-septanoside (26) and 1,5-Anhydro-3,4,7-tri-*O*-benzyl-α-D-*glycero*-D-*galacto*-septanose (27). To a solution of oxepine **4** (0.2 g, 0.37 mmol) in DCM (20 mL) was added DMDO (2.44 mL, 0.22 M) at 0 °C and the mixture was stirred for 1 h. Volatiles were removed under

reduced pressure and ^{1}H NMR showed quantitative conversion with formation of a mixture of products. The residue was dissolved in CH_3OH (10 mL) and $NaOCH_3$ (15 mg) was added. The mixture was stirred at rt for 12 h and then quenched by adding saturated NH_4Cl (3 mL). The solvent was removed under reduced pressure and H_2O (15 mL) was added to the mixture. Extraction with DCM (3 × 10 mL), drying, removal of solvent, and purification by column chromatography gave two products. The first eluted with hexanes/ethyl acetate = 9/1 giving **26** (0.12 g, 55%) as a thick liquid. R_f = 0.55 (hexanes:EtOAc 7:3). $[\alpha]_D^{22}$ +55.91 (*c* 2.28, CHCl$_3$). ^{1}H NMR (300 MHz, CDCl$_3$) δ 2.67 (d, *J* = 4.2 Hz, D$_2$O exchangeable, 1H), 3.45 (s, 3H), 3.60 (d, *J* = 4.1 Hz, 2H), 3.78 (dd, *J* = 9.3, 5.8 Hz, 1H), 3.94 (d, *J* = 7.7 Hz, 1H), 3.98–4.04 (m, 2H), 4.10 (dt, *J* = 7.6, 3.8 Hz, 1H), 4.31 (d, *J* = 11.2 Hz, 1H), 4.44 (d, *J* = 12.2 Hz, 1H), 4.54 (d, *J* = 12.2 Hz, 1H), 4.55 (d, *J* = 11.2 Hz, 1H), 4.64 (d, *J* = 11.9 Hz, 1H), 4.71 (s, 2H), 4.73 (d, *J* = 11.9 Hz, 1H), 4.88 (d, *J* = 3.5 Hz, 1H), 7.08–7.20 (m, 2H), 7.24–7.38 (m, 18H); ^{13}C NMR (75 MHz, CDCl$_3$) δ 55.7, 70.3, 71.0, 71.4, 73.1, 73.2, 73.4, 73.5, 77.4, 77.9, 79.7, 98.4, 127.4 (s), 127.5 (s), 127.54 (s), 127.6 (s), 127.7 (s), 127.8 (s), 128.0 (s), 128.2 (s), 128.23 (s), 128.3 (s), 138.0, 138.1, 138.3, 138.5. ESI-MS *m/z* (M + Na)$^+$ calcd for C$_{36}$H$_{40}$O$_7$Na$^+$ 607.2666, found 206.2671. Further elution with hexanes:EtOAc (8.5:1.5) gave **27** (0.05 g, 29%) as a thick liquid. R_f 0.59 (hexanes:EtOAc 7:3). $[\alpha]_D^{22}$ +67.54 (*c* 2.0, CHCl$_3$). ^{1}H NMR (300 MHz, CDCl$_3$) δ 2.48 (d, *J* = 4.7 Hz, D$_2$O exchangeable, 1H), 3.56 (dd, *J* = 10.8, 4.7 Hz, 1H), 3.62 (dd, *J* = 10.8, 2.0 Hz, 1H), 3.69 (dd, *J* = 9.7, 4.3 Hz, 1H), 3.85 (m, 1H), 4.07 (d, *J* = 2.2 Hz, 1H), 4.25–4.31 (m, 1H), 4.36 (d, *J* = 4.3 Hz, 1H), 4.40 (d, *J* = 11.6 Hz, 1H), 4.45 (d, *J* = 12.3 Hz, 1H), 4.49 (d, *J* = 11.5 Hz, 1H), 4.51 (d, *J* = 11.5 Hz, 1H), 4.60 (d, *J* = 11.4 Hz, 1H), 4.61 (d, *J* = 12.6 Hz, 1H), 5.27 (d, *J* = 4.6 Hz, 1H), 7.14–7.35 (m, 15H); ^{13}C NMR (75 MHz, CDCl$_3$) δ 69.2, 70.3, 71.3, 72.2, 73.4, 73.7, 79.6, 79.7, 82.9, 98.7, 127.6 (s), 127.8 (s), 127.83 (s), 127.9 (s), 128.0, 128.3 (s), 128.4 (s), 128.5 (s), 137.5 (s), 137.6, 137.9. ESI-MS *m/z* (M + Na)$^+$ calcd for C$_{28}$H$_{30}$O$_6$Na$^+$ 485.1935, found 485.1929.

2-*O*-Acetyl-3,4,5,7-tetra-*O*-benzylmethyl-α-D-*glycero*-D-*galacto*-septanoside (26a). To a solution of **26** (0.09 g, 0.154 mmol) in pyridine (0.12 g, 1.54 mmol) was added Ac$_2$O (0.47 g, 4.6 mmol) and DMAP (5 mg). The mixture was stirred for 15 h at rt and volatiles were removed under reduced pressure. The residue was purified by column chromatography (hexanes/ethyl acetate = 9/1) giving **26a** (0.09 g, 93%) as a thick liquid. R_f 0.49 (hexanes:EtOAc 7:3); $[\alpha]_D^{22}$ +34.70 (*c* 1.5, CHCl$_3$). ^{1}H NMR (300 MHz, CDCl$_3$) δ 2.01 (s, 3H), 3.39 (s, 3H), 3.57 (dd, *J* = 10.4, 2.6 Hz, 1H), 3.63 (dd, *J* = 10.4, 5.1 Hz, 1H), 3.84 (dd, *J* = 8.9, 6.1 Hz, 1H), 3.85–3.92 (m, 2H), 3.93–4.00 (m, 1H), 4.31 (d, *J* = 11.2 Hz, 1H), 4.41 (d, *J* = 12.1 Hz, 1H), 4.52 (d, *J* = 11.2 Hz, 1H), 4.56 (d, *J* = 11.2 Hz, 1H), 4.70 (s, 2H), 4.73 (s, 2H), 4.94 (d, *J* = 3.2 Hz, 1H), 5.34 (dd, *J* = 7.5, 3.2 Hz, 1H), 7.10–7.34 (m, 20H); ^{13}C NMR (75 MHz, CDCl$_3$) δ 21.0, 55.9, 70.9, 71.0, 72.1, 73.1, 73.3, 73.48, 73.53, 76.7, 76.8, 79.4, 97.2, 127.5, 127.52, 127.54, 127.6, 127.7 (s), 128.1 (s), 128.2 (s), 128.3 (s), 138.0, 138.1, 138.3 (s). ESI-MS *m/z* (M + Na)$^+$ calcd for C$_{38}$H$_{42}$O$_8$Na$^+$ 649.2772, found 649.2775.

1,5-Anhydro-3,4,7-tri-*O*-benzyl-α-D-*glycero*-D-*galacto*-septanose (27a). To a solution of **27** (0.06 g, 0.13 mmol) in pyridine (0.5 mL) was added Ac$_2$O (2 mL) and DMAP (2 mg) and the mixture was stirred at rt for 15 h. Volatiles were removed under reduced pressure and the material was purified by column chromatography (hexanes:EtOAc 9:1) to give **27a** (0.058 g, 89%) as a thick liquid. R_f 0.47 (hexanes:EtOAc 8:2); $[\alpha]_D^{22}$ +99.85 (*c* 1.06, CHCl$_3$). ^{1}H NMR (300 MHz, CDCl$_3$) δ 2.06 (s, 3H), 3.60 (br s, 2H), 3.75 (br d, *J* = 1.3 Hz, 2H), 4.28 (d, *J* = 2.2 Hz, 1H), 4.41 (br s, 1H), 4.43 (d, *J* = 11.4 Hz, 1H), 4.44 (d, *J* = 11.9 Hz, 1H), 4.51 (s, 2H), 4.57 (d, *J* = 13.0 Hz, 1H), 4.61 (d, *J* = 12.2 Hz, 1H), 5.08 (dd, *J* = 4.4, 2.2 Hz, 1H), 5.58 (d, *J* = 4.4 Hz, 1H), 7.05–7.23 (m, 2H), 7.25–7.46 (m, 13H); ^{13}C NMR (75 MHz, CDCl$_3$) δ 20.6, 68.9, 70.1, 71.4, 72.4, 73.3, 73.9, 79.1, 79.9, 80.2, 96.9, 127.8 (s),

127.85 (s), 127.9 (s), 128.1 (s), 128.3 (s), 128.4 (s), 128.5 (s), 137.3, 137.4, 138.1, 169.8. ESI-MS *m/z* (M + Na)$^+$ calcd for C$_{30}$H$_{32}$O$_7$Na$^+$ 527.2040, found 527.2042.

Methyl-3,4;5,7-diacetonide-β-D-*glycero*-D-*galacto*-septanoside (29). To a solution of oxepine **28** (0.04 g, 0.156 mmol) in DCM (10 mL) was added DMDO (0.53 mL, 0.36 M) at 0 °C and the mixture was stirred for 1 h. Volatiles removed under reduced pressure and ^{1}H NMR of the residue showed quantitative conversion of **28**. This material was dissolved in CH_3OH (5 mL) and $NaOCH_3$ (7 mg) was added. The reaction was stirred overnight and quenched by adding saturated NH_4Cl (2 mL). Volatiles were removed under reduced pressure and H_2O (15 mL) was added to the residue. Extraction with DCM (3 × 10 mL), drying of the DCM layers, and removal of solvent under reduced pressure was followed by purification via column chromatography (hexanes/ethyl acetate = 4/6) to give **29** (0.04 g, 84% for 2 steps) as a white solid. R_f 0.49 (hexanes:EtOAc 2:8). Mp 96–98 °C. ^{1}H NMR (400 MHz, CDCl$_3$) δ 1.35 (s, 6H), 1.41 (s, 3H), 1.48 (s, 3H), 2.42–2.59 (br s, D$_2$O exchangeable, 1H), 3.47 (m, 1H), 3.50 (s, 3H), 3.63 (d, *J* = 8.0 Hz, 1H), 4.01–4.10 (m, 4H), 4.21 (d, *J* = 8.0 Hz, 1H), 4.37 (q, *J* = 8.0 Hz, 1H); ^{13}C NMR (100 MHz, CDCl$_3$) δ 25.4, 26.4, 26.9, 28.1, 56.9, 66.6, 73.2, 73.5, 73.7, 74.2, 78.7, 103.4, 109.4, 110.3. ESI-MS *m/z* (M + Na)$^+$ calcd for C$_{14}$H$_{24}$O$_7$Na$^+$ 327.1414, found 327.1410.

Methyl-β-D-*glycero*-L-*manno*-septanoside (25b). To a solution of **25** (0.15 g, 0.26 mmol) in CH_3OH (15 mL) was added Pd(OH)$_2$ (0.17 g, 1.23 mmol) and the solution was stirred under H$_2$ (1 atm) for 3 h. The catalyst was filtered through a pad of celite and the filtrate was concentrated under reduced pressure to give a thick liquid (0.054 g, 95%). R_f 0.54 (DCM:CH$_3$OH 9:1). $[\alpha]_D^{22}$ +6.0 (*c* 1.4, CH$_3$OH). ^{1}H NMR (400 MHz, CD$_3$OD) δ 3.41 (s, 3H, –OCH$_3$), 3.61–3.66 (m, 3H), 3.70 (dd, *J* = 12.3, 8.2 Hz, 1H), 3.86 (dd, *J* = 2.8, 2.8 Hz, 1H), 3.91 (d, *J* = 1.8 Hz, 1H), 3.99 (dd, *J* = 9.5, 3.7 Hz, 1H), 4.31 (d, *J* = 4.8 Hz, 1H); ^{13}C NMR (100 MHz, CD$_3$OD) δ 56.8, 63.3, 68.8, 71.7, 72.8, 76.2, 80.3, 110.1. ESI-MS (M + Na$^+$) calcd for C$_8$H$_{16}$O$_7$Na$^+$ 247.0794, found 247.0796.

Methyl-α-D-*glycero*-D-*galacto*-septanoside (26b). To a solution of **26** (0.1 g, 0.17 mmol) in CH_3OH (10 mL) was added Pd(OH)$_2$ (0.115 g, 0.82 mmol) and the solution was stirred under H$_2$ (1 atm) for 4 h. Catalyst was filtered through a pad of celite and the filtrate was concentrated under reduced pressure to give **26b** as a thick liquid (0.036 g, 94%). R_f 0.52 (DCM:CH$_3$OH 9:1). $[\alpha]_D^{22}$ +57.31 (*c* 1.5, CH$_3$OH). ^{1}H NMR (400 MHz, CD$_3$OD) δ 3.43 (s, 3H), 3.60 (dd, *J* = 8.8, 7.7 Hz, 1H), 3.65 (dd, *J* = 12.0, 7.0 Hz, 1H), 3.74 (dd, *J* = 12.0, 3.0 Hz, 1H), 3.74–3.77 (m, 1H), 3.84 (d, *J* = 1.8 Hz, 1H), 3.86 (d, *J* = 3.0 Hz, 1H), 3.96 (dd, *J* = 6.8, 2.2 Hz, 1H), 4.67 (d, *J* = 3.0 Hz, 1H); ^{13}C NMR (100 MHz, CD$_3$OD) δ 56.4, 64.3, 71.6, 73.2, 73.3, 75.3, 75.6, 100.1. ESI-MS (M + Na$^+$) calcd for C$_8$H$_{16}$O$_7$Na$^+$ 247.0794, found 247.0783.

Methyl-β-D-*glycero*-D-*galacto*-septanoside (29b). To a solution of **29** (0.16 g, 0.526 mmol) in EtOH/H$_2$O (32 mL, 1:3) was added Amberlite-IR-120 (260 mg) then the solution was refluxed at 110 °C for 3.5 h. The reaction mixture was cooled and filtered through a pad of celite and the filtrate was concentrated under reduced pressure to give **29b** (0.11 g, 93%) as an oil. R_f 0.35 (DCM:CH$_3$OH 8:2). $[\alpha]_D^{22}$ –13.97 (*c* 1.4, CH$_3$OH). ^{1}H NMR (300 MHz, CD$_3$OD) δ 3.34–3.44 (m, 1H), 3.48 (s, 3H), 3.60–3.3.74 (m, 3H), 3.76–3.88 (m, 3H), 4.22 (d, *J* = 7.2 Hz, 1H); ^{13}C NMR (75 MHz, CD$_3$OD) δ 56.7, 64.6, 71.8, 76.2, 76.3, 76.4, 84.5, 110.8. ESI-MS (M + Na$^+$) calcd for C$_8$H$_{16}$O$_7$Na$^+$ 247.0794, found 247.0773.

Computational Methods. A Monte–Carlo conformational search (torsional sampling: 5000 steps; energy window for saving structures: 50 kJ/mol) was used to generate the conformers of **2a**, **3a**, and **4a**. The calculations were performed by employing the OPLS-AA force field[36] as implemented in the MacroModel software (version 8.5)[37] from Schrödinger. This process resulted in 431 unique conformations for **2a**, 655 unique conformations for **3a**, and 750 unique conformations for **4a**.

The 20 most stable conformers of **2a**, 25 most stable conformers of **3a**, and 43 most stable conformers of **4a** from the OPLS-AA conformational searches were further optimized at the B3LYP/6-31G* level of theory.[28–31] All density functional theory (DFT) calculations were performed with Gaussian03[38] at the Ohio Supercomputer Center. The optimized geometries and subsequently the harmonic vibrational frequencies for all of these conformers were obtained, and the relative energies were compared. A scaling factor of 0.9806[45] was used for the zero-point vibrational energy (ZPE) corrections. Enthalpies and free energies were obtained from the calculated thermal and entropic corrections at 298 K, using the unscaled, harmonic vibrational frequencies for the vibrational contribution to the partition function. After this analysis, 4 conformations for **2a**, 3 conformations for **3a**, and 5 conformations for **4a** were obtained, and for which their relative free energies were within ∼1 kcal/mol of the global minimum in each case.

The transition states for the epoxidation by DMDO with 10 different conformers of **2a**, **3a**, and **4a** were located at the B3LYP/6-31G* level of theory. Transition state structures were confirmed to have one imaginary vibrational frequency. The desired reactants and products were located by displacement (10%) of the transition state geometries along the normal coordinate of the imaginary vibrational frequency in the positive and negative directions, followed by careful optimization with the analytical second derivatives (opt = calcfc).

Single-point energy and natural population analysis (NPA)[42] calculations were then performed for these stationary points at the B3LYP/6-31+G** level of theory with six Cartesian d functions. The effect of solvation on the gas-phase single-point calculations was investigated by using the polarizable continuum model (PCM)[32–35] for CH_2Cl_2 and CH_3OH as solvents.

The electrostatic potential for each of the most stable conformers of **2a**, **3a**, and **4a** (**2a**-A, **3a**-A, and **4a**-A, respectively) was generated with Gaussview 3.0[46] at the B3LYP/6-31G* level of theory in the gas phase. The isosurface value was 0.02 au.

Supporting Information Available: NMR spectra for all new compounds and a summary of enthalpic and free energies, optimized geometries, vibrational frequencies, as well as NPA results for each conformer, reactant complex, transition state and product. This material is available free of charge via the Internet at http://pubs.acs.org. Complete crystallographic data for the structural analysis of methyl septanoside **29** have been deposited in the Cambridge Crystallographic Data Centre (CCDC), No. 655858; copies of this information may be obtained free of charge from CCDC, 12 Union Road, Cambridge CB2 1EZ, UK (Fax: +44−1223−336033; web: www.ccdc.cam.ac.uk/conts/retrieving/html; e-mail: deposit@ccdc.cam.ac.uk).

JO800979A

(45) National Institute of Standards and Technology, Computational Chemistry Comparison and Benchmark Database Release 12, 2005.

(46) Copyright 2000−2003 by Semichem, Inc.